2017-01-01

Investigation Into The Role Of N-Terminal Acetylation Of Esat-6 In Pathogenesis Of Mycobacterium Tuberculosis

Javier A. Aguilera
University of Texas at El Paso, jaguilera5@miners.utep.edu

INVESTIGATION INTO THE ROLE OF N-TERMINAL ACETYLATION OF ESAT-6 IN PATHOGENESIS OF *MYCOBACTERIUM TUBERCULOSIS*

JAVIER A. AGUILERA

Master's Program of Biological Sciences

APPROVED:

Jianjun Sun, Ph.D., Chair

Hugues Ouellet, Ph.D.

Chuan Xiao, Ph.D.

Charles Ambler, Ph.D.

Dean of the Graduate School

INVESTIGATION INTO THE ROLE OF N-TERMINAL ACETYLATION OF ESAT-6 IN PATHOGENESIS OF *MYCOBACTERIUM TUBERCULOSIS*

by

JAVIER A. AGUILERA, B.S.

THESIS

Presented to the Faculty of the Graduate School of

The University of Texas at El Paso

in Partial Fulfillment

of the Requirements

for the Degree of

MASTER OF SCIENCE

Department of Biological Sciences

THE UNIVERSITY OF TEXAS AT EL PASO

May 2017

Acknowledgements

This work was supported by the National Institutes of Health Grant 5G12RR008124 from the National Center for Research Resources and Grant 2G12MD007592 from National Institutes on Minority Health Disparities, a component of National Institutes of Health. This Research is also supported by University of Texas at El Paso new faculty start-up funds.

Abstract

Mycobacterium tuberculosis (Mtb), the causative agent for the disease Tuberculosis (TB) in humans, is present as a latent infection in approximately one third of the world's population. Mtb has become more resilient over the years. The vaccine, *Mycobacterium bovis* bacillus Calmette-Guerin (BCG), loses effectiveness 10 years after initial vaccination. Recent research has found 6-kD early secretory antigenic target (ESAT-6) and 10-kD culture filtrate protein (CFP-10) are secreted as a heterodimer by Mtb and play important roles in virulence. Additionally, ESAT-6 has been determined to contain membrane lytic activity while CFP-10 has been suggested to be a molecular chaperone. Studies suggest ESAT-6 dissociates from CFP-10 at low pH to interact with the phagosomal membrane, which facilitates the translocation of Mtb into the cytosol of a macrophage. Furthermore, membrane lytic ability of ESAT-6 only occurs after it dissociates from CFP-10. However, the mechanism of heterodimer dissociation remains elusive. Previous studies have identified and isolated an N-α-terminally acetylated ESAT-6 protein. Binding affinity between CFP-10 and ESAT-6 is greatly reduced after acetylation, suggesting that N-α-terminal acetylation could be the cause for the dissociation of the ESAT-6/CFP-10 heterodimer. In this study, we aim to determine whether N-α-terminal acetylation of Threonine-2 (T2) on ESAT-6 is required for dissociation of the heterodimer. To test this, we replaced T2 with three different amino acids alanine (T2/A), glutamine (T2/Q), and arginine (T2/R). We hypothesized T2/A and T2/Q would function as acetylation-mimicking residues with similar activity to wild-type ESAT-6, while T2/R serves as acetylation negative control with less activity. Preliminary data, a liposome leakage assay with the dye/quencher pair, 8-aminonaphthalene-1,3,6 trisulfonic acid (ANTS) and p-xylene-bis-pyridinium bromide (DPX), revealed that all of

these mutations did not affect pore formation of ESAT-6 alone, but diminished pore formation of the ESAT-6 complexed with CFP-10. This data suggested T2/A, T2/Q and T2/R mutations inhibited heterodimer dissociation, prompting generation of a new T2/S mutant. Cytotoxicity analysis of macrophages infected by *Mycobacterium marinum* revealed decreased activity in the mutants while complemented strains with WT ESAT-6 or T2/S ESAT-6 recovered activity. As expected, the mutations inhibited the cytosolic translocation as measured by CCF4 fluorescence resonance energy transfer (FRET). The change in virulence was presumed to be due to the lack of acetylation in the T2/Q, T2/R, and T2/A mutants. Isolation of acetylated ESAT-6 was achieved via ASB-14 or 6M guanidine and was confirmed via 4-chloro-7-nitrobenzofurazan (NBD-Cl) and mass spectrometry. Native gel shift assay revealed un-acetylated ESAT-6 to form a complex with CFP-10 more efficiently than acetylated ESAT-6. Furthermore, preliminary studies using surface plasmon resonance revealed differential binding affinity between either specie of ESAT6. This study has revealed the physiological importance of N-α-acetylation of ESAT-6 in Mtb infection.

Table of Contents

List of Tables

List of Figures

Chapter 1: Introduction

Mycobacterium tuberculosis (Mtb) is the causative agent for tuberculosis (TB), a disease present as a latent state in approximately one third of the world population (Zumla, 2014; WHO, 2016). The disease is responsible for over 1 million deaths each year (CDC, 2015). Much progress has been made in understanding the mechanisms of Mtb infection. Previous reports show that Mtb is internalized by a macrophage into a phagosome; however, the pathogen is capable of translocation from phagolysosome into the cytosol of an infected macrophage (Van Der Wel, N. 2007). It has been well established that the complex named ESX-1 is important in Mtb pathogenesis. The ESX-1 complex mediates the secretion of 6-kD early secretory antigenic target (ESAT-6) and 10-kD culture filtrate protein (CFP-10), two proteins secreted as a heterodimer (Fortune, S., 2005), which allow Mtb to rupture the phagosome and translocate into the cytosol of the host cell (Houben, D., 2012; Smith, J., 2008; Renshaw, P.S., 2002).

1.1 Facts and Statistics

Mtb is one of the leading causes of death worldwide; approximately 9.6 million people were estimated to have fallen ill with TB in 2014 (Dolin 1994, CDC, 2016). Quick progression of the disease was observed in 2015, where the numbers rose to a total 10.4 million people becoming sick with the disease and 1.8 million people dying from TB-related deaths (CDC, 2016). TB is most prevalent in underdeveloped countries such as those found in Africa. A more particular threat in that region exists with co-infection with HIV and TB. An estimated 1.2 million people were co-infected with HIV and Mtb. Approximately a third of the deaths caused by HIV are a result of TB (Komrower, 2015;

Venturini, 2015). Furthermore, drug resistant TB has shown an increase in incidence with approximately 480,000 cases of drug resistant TB in 2015. (CDC, 2016) TB is one of the leading causes of death in the world, having surpassed even HIV, prompting the urgency to develop better therapeutic options. Though the disease has caused shiver inducing death numbers, it is important to note that millions of cases have been treated successfully. Continued growth and dedication from the scientific field is essential to the abolishment of the disease.

1.2 Treatment of a Typical Mtb Infection

Mtb is a very resilient bacterium that requires a long antibiotic treatment regimen. The typical treatment of TB disease includes a cocktail of four antibiotics that are taken for six to nine months and sometimes longer. The core antibiotic treatment includes isoniazid, rifampin, ethambutol, and pyrazinamide. The typical treatment regimen includes daily intake of the four antibiotics for 8 weeks. After 8 weeks, the dose is lowered to a daily intake of isoniazid and rifampin for 18 weeks, or intake of isoniazid and rifampin twice per week for 18 weeks (CDC, 2016). Resolution of the disease is often observed after the 18 week treatment, though in certain occasions the treatment may be longer. Mycobacteriaare highly prone to gaining antibiotic resistance, and thus treatment regimens require very attentive and consistent dosage.

1.3 Rise of Antibiotic Resistant TB Defines New Borders

A particularly alarming occurrence, which is becoming more frequent, is the development of drug resistant TB. Patients at risk of developing drug resistant TB include those who do not take their antibiotics regularly, do not take all of their TB drugs, use

drugs of poor quality, or develop TB disease again amongst other reasons. As defined by the WHO there are different types of drug resistant TB. Multidrug-Resistant TB (MDR-TB) is resistant to isoniazid and rifampin, and Extensively Drug-Resistant TB (XDR-TB) is resistant to isoniazid, rifampin, any fluoroquinolone, and at least one injectable second line drug. (CDC, 2006) Not yet defined by the WHO, cases of Totally Drug-Resistant TB (TDR-TB) have been reported (Velayati, A., 2009; Udwadia, Z. F., 2012, Klopper 2013). These strains appear to have developed resistance to every possible treatment option. The development of any drug resistant strain is a serious matter that progresses quickly. MDR-TB is now seen in approximately 5% of cases, while at least 40,000 cases of XDR-TB occur every year. Progression of antibiotic resistance could ~~revert~~ bring back humanity into a pre-antibiotic era. For this same reason, research for the rapid development of new therapeutics against TB is crucial.

1.4 Regions of Difference Give Insight on Virulent Genes

The advancement of genomic studies serves an instrumental role in identifying genes essential for pathogenic bacteria. As has been well established, co-evolution between host and pathogen favors the adaptation of pathogen to host immunities. These specific alterations in the genome of a pathogen become imperative to the pathogen's survival. The genes responsible for the virulence of a pathogen in a host have been appropriately termed virulent genes. The successful identification and inhibition of the virulent genes comprise a potential therapeutic target. Comparative analyses between virulent species of mycobacteria have illustrated 14 regions of difference (RD1-14), which have been implicated in recent studies (Gordon, 1999; Behr 1999). As expected, genome-wide analysis revealed the H37Rv Mtb strain to contain RD1-14, while the

attenuated *M. bovis var.* BCG strain lacks them. Furthermore, another 6 regions H37Rv deletion 1-5 (RvD1-5) as well as Mtb*.* specific deletion 1 (TBD1) have been identified (Brosch 1999). All of these regions code for a variety of virulent factors, conferring Mtb its fundamental systems to thrive as a pathogen. As expected, targeting these genes is a major point of interest for the development of novel therapeutics.

1.5 Key Mechanisms for Mtb Pathogenesis

Mtb possesses many qualities that make it a successful pathogen. These qualities include the intricate cell wall accessorized by complex lipids. Ancillary to a strong cell wall Mtb has the ability to arrest phagosomal maturation in a macrophage (Chua 2004; Hoffman 2017), resistance to reactive nitrogen species (RNS) and reactive oxygen species (ROS) (Piddington, 2001; Kendall, 2004; Voskuil, 2003), adaption for catabolism (McKinney, 2000; Segal, 1956; Pandey, 2008), and the secretion of important virulence factors (Conrad, 2017; Abdallah 2007). All of these key properties of Mtb are what makes it such a strong pathogen.

The cell envelope of mycobacteria is composed of an intricate cell wall with complex lipids; it consists of an inner membrane, peptidoglycan and arabonigalactan layers, a mycolic acid layer and an outer capsular layer. The cell wall of Mtb has been shown to contain over 500 proteins, out of which 150 outer membrane proteins have been identified as important virulence factors (Wolf, 2010), the role of these proteins varies from transfer and synthesis of sugars and other molecules (Murphy, 2005; Senaratne, 1998; Braibant, 2000), or serving as ligands (Casali, 2007). A strong cell envelope accessorized by complex lipids is essential for Mtb’s survival.

Complex lipids are characteristic of mycobacteria many of which are adaptive effectors of virulence. Fortifying the tough cell wall of mycobacteria are the mycolic acids: trehalose monomycolates (TMM) and trehalose dimycolates (TDM) which are covalently attached to arabinogalactan and sterified to glycerol and trehalose (Brennan, 1995). Furthermore, additional lipids and glycolipids include di-acylated trehaloses(DAT), tri-acylated trehaloses(TAT), poly-acyltrehaloses (PAT), sulfolipids (SL), phthiocerol dimycocerosates (PDIM), and found in hypervirulent strains of Mtb, phenolic glycolipids (PGL) (Mamadou, 1997; Jia 2012). All of these complex lipids have key roles in Mtb virulence, and have been suggested to work in essential pathways of infection.

Although Mtb possesses a plethora of lipids, of its own, another key element is its ability to use other lipids or compounds as a carbon source. Mtb is capable of metabolizing fatty acids, lipids and cholesterol. Metabolizing fatty acids and lipids has been implied to play a role in the ability for Mtb extra-pulmonary infection (Rindi 2002). Catabolism of cholesterol has been one of the most surprising properties innate to Mtb and has served as a therapeutic target (Miner, 2009; Hughes, 2011). A sophisticated network of protein interactions makes this pathway possible for Mtb, and cholesterol plays a crucial role for the synthesis of PDIM (Pandey, 2008; Griffin 2011).

Some of the properties of Mtb, particularly those originating from the fortified cell envelope, confer the pathogen resistance to macrophage offensive action. Mtb has shown resistance to RNS or ROS (Voskuil, 2011; Cirrillo 2009). Macrophages generally produce ROS and RNS which contain powerful bactericidal properties. Mtb has developed unique pathways that allow resistance to these anti-bacterial compounds. Some virulence factors expressed by Mtb allow for the breakdown of ROS/RNS, while

others provide the bacteria with tolerance (Piddington, 2001; Voskuil 2003). Ability of the pathogen to resist macrophage action is extremely relevant to TB research.

Similarly, another key characteristic of Mtb is its ability to arrest phagosomal maturation. (Vergne, 2004) In a typical infection, the first line defensive cell of the human body, the macrophage, phagocytizes pathogens into a phagosomal compartment. The phagosome will then fuse with lysosomes to turn into a phagolysosome. This fusion is normally a death sentence for a pathogen; however Mtb has evolved mechanisms that inhibit this action. Some key virulence factors of Mtb have been shown to inhibit the recruitment of effectors to phagosomes, or inhibit acidification of the phagosome (Sun, 2010; Wong, 2011; Iantomasi, 2012). The pathogen is then capable of translocating from the phagosome into the cytosol through a number of pathways not yet well understood where Mtb is capable of continuing infection.

More relevant to the line of research in this project, Mtb also makes use of a wide array of secreted proteins. Mtb has been shown to contain many different secretion systems, but more importantly the type II and type VII secretion systems have been implied to have a key role in virulence of the pathogen (Abdallah, 2007). Moreover, the mycobacterial specific type VII secretion system has been particularly well studied and includes five homologous secretion systems termed ESX 1-5 (Houben, 2014). Out of these 5, ESX-1 and ESX-5 have been correlated with virulence of Mtb. The ESX-1 secretion system is the most heavily researched of these and consists of two effector proteins 6-kDa Early Secretory Antigenic Target (ESAT-6) and 10-kDa culture filtrate protein (CFP-10), whose interaction is the key topic of this thesis (Simeone, 2009).

1.6 Secretion Systems of Mtb Contain Essential Virulence Factors

The type VII secretion system contains ESX-1, which is a key secretion system for Mtb. The two effector proteins ESAT-6 and CFP-10, collectively known as esx-1 have been demonstrated to be vital virulence factors (Sørensen, 2009). Also located within the ESX-1 are auxiliary proteins including EccA, EccB, EccC, EccD, EspA, EspB, EspC, and EspD proteins whose role has not been studied quite as well as the effector proteins (Stoop, 2012; Wirth, 2012; Rosenberg, 2015). Interestingly interdependence for each other was found between secreted proteins of ESX-1, if ESAT-6 is deleted EspB could also be affected. More meaningful to the collective virulence of these genes, their localization in RD1 implies their relevance. When RD1 was removed from virulent strains of Mtb, attenuation of these strains occurred (Pym, 2002). Moreover, complementation of RD1 to non-pathogenic BCG strains showed restored virulence (Kristi 2004). Furthermore, complementation of BCG with ESAT-6 conferred better immunities of the vaccine strain (Pym, 2003; Groschel, 2017). It is specifically for these reasons that many studies have focused their efforts into this gene and have established a portion of its role. Many different roles have been tied to esx-1 which include phagosomal maturation arrest (Tan, 2006), cytosolic translocation of Mtb (van der Wel, 2007; Houben, 2012), and has been implied to take a role in a DNA sensing pathway (Watson, 2012) or synergize with other virulence factors such as PDIM (Augenstreich, 2017). The exact role has not been fully elucidated, but it is very clear that esx-1 has a key role in cytosolic translocation of Mtb. Without a doubt, the esx-1 is a very important virulence factor of Mtb.

1.7 Esx-1 Confers Essential Virulent Properties to Mtb

ESAT-6, accompanied by CFP-10, is responsible for membrane cell-lysis (Houben, D., 2012; de Jonge, M. I., 2007). Studies have shown that BCG lacks both

ESAT-6 and CFP-10 and is not able to rupture the phagosome membranes in macrophages, suggesting that ESAT-6 is a determining factor for Mtb pathogenesis. (Brosch, R. 2007; Mahairas, G., 1996; Berh, M. A., 1999). Additionally, it was determined that CFP-10 does not contain membrane-lytic activity, rather it is an intrinsic property of ESAT-6 alone; CFP-10 behaves as a molecular chaperone of ESAT-6 (de Jonge, M. I., 2007). Current studies have proposed that under acidic condition ESAT-6 is dissociated from CFP-10, an essential step for ESAT-6 to interact with the membrane. (de Leon, J., 2012; de Jonge, M. I., 2007) However, the mechanism of ESAT-6/CFP-10 dissociation remains unclear.

1.8 General Structure and Interaction of the ESAT-6 and CFP-10 Complex

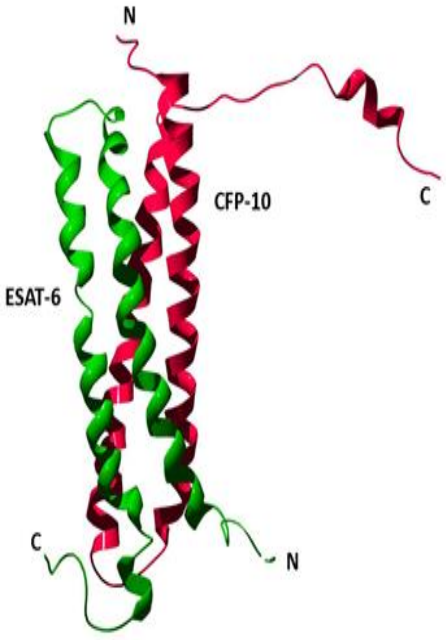

Figure 1: Solution structure of ESAT-6 and CFP-10 complex (Protein Data Bank ID 1WA8)

The structure for CFP-10 and ESAT-6 is formed by two helical hairpin structures composed of a helix, bridge, and another helix with C- and N-terminal flexible arms. The helices have extensive hydrophobic surfaces. Interaction of the two proteins is based on van der Waals contacts, while two salt bridges stabilize the N-terminal helix-1 of CFP-10 to the C-terminal helix-2 of ESAT-6, and the C-terminal helix-2 of CFP-10 to N-terminal ESAT-6 helix-1 (Renshaw, P. S. 2005). . The length of helices 1 and 2 from ESAT-6 were measured to be ~50 Å spanning the depth of a typical membrane,

and C- and N- terminal flexible arms have been shown essential for membrane disruption of ESAT-6 (Ma, Y., 2015).

1.9 Specific Mechanism of Action of ESAT-6 and CFP-10 Remains Elusive

Though the *esx-1* complex has been heavily researched in the past decades, there is still much debate within the scientific community of its exact mechanism of action. Previous research has suggested CFP-10 to function as a molecular chaperone. ESAT-6 and CFP-10 form a tight 1:1 heterodimer. Dissociation of this complex must occur before ESAT-6 is capable of membrane lysis. The mechanism underlying dissociation remains elusive. In spite of all controversy, it is clear that ESAT-6 is essential for cytosolic translocation of Mtb. It appears that acidification of the protein prompts or plays an important role in the dissociation of the heterodimer complex (de Jonge M. I., 2007), as it has shown to prompt increased folding and organization via more α-helical structure of ESAT-6 (Ma, 2015). For this reason and others, lowering the pH has been implied to serve as a trigger for the dissociation of ESAT-6 from its molecular, citing the conditions found within a macrophage. (Kupz, 2016; Zhang, 2016) Others have found evidence to suggest differently. (Conrad, 2017). However, different preparations of ESAT-6 might determine the discrepancy between the results of different research groups. Some groups prepared their ESAT-6 proteins via expression in *E. coli* versus other groups preparing ESAT-6 in *M. smegmatis*. Preparations in *E. coli* resulted in a protein that lacked N-α-terminal acetylation while those in *M. smegmatis* resulted in a protein that contained this type of acetylation and may be important for the dissociation of the heterodimer complex.

1.10 Acetylation at the N-terminus Could Be the Driving Factor For the pH-Dependent Dissociation of the Heterodimer Complex

An earlier report showed ESAT-6 is acetylated at its N-terminus in mycobacteria, and displayed differential binding to its un-acetylated version (Okkels, L. M., 2004). ESAT-6 has been implicated as a unique virulence factor capable of N-α-terminal acetylation (Lange S., 2014). The importance of acetylation was observed in another study (Medie, F. M., 2014), where an inverse correlation between the virulence of *M. marinum* and the acetylation of ESAT-6 was proposed. It was previously observed by (de Jonge, M. I., 2007) that ESAT-6 is incapable of interacting with the membrane when it forms a complex with CFP-10. Given these premises, we hypothesize that N-α-acetylation of ESAT-6 at the second residue, threonine-2 (T2), is essential for the dissociation of the heterodimer complex.

Chapter 2: Specific Aims

2.1 Determine the Effects of Mutations at T2 of ESAT-6.

For this portion of the project, various mutations were generated in ESAT-6. These mutations will be used to compare the lysing ability of ESAT-6 *in vitro.* Further studies were performed *in vivo* using *M. marinum* as a model. Mutated ESAT-6 was compared in cytotoxicity of RAW 264.7 macrophages. Furthermore, ability of cytosolic translocation was compared among all strains. Appropriate control for secretion of ESAT-6 was performed as well.

2.1.1 Generate Mutations at T2 in ESAT-6 in Different Vectors

As previous literature has indicated that the ESAT-6 protein is acetylated at its N-terminal T2 residue (Okkels, 2004). To be able to effectively determine the role of acetylation at T2, mutations were introduced to replace T2 with an alanine (T2A), arginine (T2R), glutamine (T2Q), or serine (T2S). These mutations were performed in pET22B plasmid for expression and purification of ESAT-6 in BL21 *E. coli* cells, pMyNT for expression and purification of ESAT-6 complexed with CFP-10 in M1552 *M. smegmatis* cells, and pMH406 for complementation of ESAT-6 into *M. marinum.* In this study, T2S demonstrated similar function as wild type, while T2A and T2Q and T2R did not (Scroggins, 2007).

2.1.2 Determine the Effect of Mutations in ESAT-6 Towards Cell Lysing Ability

In Dr. Jianjun Sun's laboratory, a liposome leakage model has been developed for reliable detection of protein pore formation (De Leon 2012; Jacquez, 2014; Jacquez, 2015), which was used to compare the membrane lytic activity between wild-type and

mutated ESAT-6. Effects of mutations were assessed on both complexed and lone ESAT-6.

2.1.3 Determine the Effect of Mutations in Cytotoxicity of Macrophages.

To complement this data, *in vivo* infections using *M. marinum* as a model were performed in Raw264.7 macrophages. An *M. marinum* strain with a knocked out ESAT-6 gene (KO) was previously generated and is particularly useful in this study. The knock out bacteria was electroporated with ESAT-6 containing T2S, T2A, T2Q, or T2R, and wild-type ESAT-6 serving as a positive electroporation control (MmΔE6/C10(WT)). The macrophages were infected with the 5 complemented strains as well as the wild-type (WT) *M. marinum* and KO strain. The macrophages were stained with ethidium homodimer and calcein-AM, as part LIVE/DEAD viability/Cytotoxicity Kit (L3224, Molecular Probes, Eugene Oregon, USA) to compare the number of macrophages killed by WT versus the strains containing the mutated ESAT-6. The infected cells were visualized under a fluorescence microscope, with green-fluorescent cells indicating live cells and red-fluorescent cells indicating dead cells.

2.1.4 Determine the Effects of Mutations in *M. marinum* Cytosolic Translocation

Translocation of *M. marinum* from a phagosomal compartment into cytosolic space, was visualized with fluorescence resonance energy transfer (FRET) as previously described (Acosta, Y., 2014). The host cell was loaded with a chemical probe trapped within host cytoplasm, which reacts with beta βlactamase expressed in the surface of *M. marinum.* In this assay, a shift from green to blue fluorescence represents the extent at which bacteria is capable of escaping from the phagosome.

2.1.5 Control for ESAT-6 Secretion.

As a control to the *in vivo* studies, western-blotting will be used to show that the secretion of ESAT-6 from the mutated *M. marinum* strains. Mutations can be unpredictable, therefore a control to see expression of ESAT-6 is necessary. Culture filtrate was analyzed for secretion of ESAT-6 and cell lysate was analyzed for total expression.

2.2 Determine the State of N-α-acetylation and Determine its Role in the Dissociation of the ESAT-6/CFP-10 Heterodimer Complex.

To more appropriate correlate the effects of the mutation on separation between ESAT-6 and CFP-10, mutants was used to determine the whether or not the mutated proteins are acetylated. First, a method to isolate between acetylated and unacetylated types of ESAT-6 was devised and confirmed. The dissociation amongst unacetylated and acetylated types of protein was then compared.

2.2.1 Isolation of Acetylated ESAT-6.

To effectively determine if acetylation is the cause for dissociation of the ESAT-6/CFP-10 complex, the state of acetylation must be compared between mutant ESAT-6 and WT ESAT-6. To isolate the acetylated ESAT-6, the protein was co-purifed as a heterodimer with ESAT-6 and then dissociated via detergent or high concentrations of guanidine (Renshaw, P. S., 2002; Refai, A., 2015).

2.2.2 Determination of Acetylation States of ESAT-6.

The state of acetylation was determined using 4-chloro-7-nitrobenzofurazan (NBD-Cl). As shown in a previous literature (Bernal-Perez, 2012), NBD-Cl binds to the non-acetylated N-α-terminal amine group of protein, and upon binding it emits fluorescence, while it does not bind to the N-α-terminal ~~N-terminal~~ amine group due to the presence of N-α-acetylation, which makes it a reliable method to measure acetylation state. It is expected that mutated proteins incapable of acetylation will have a higher fluorescence, while proteins containing N-α-acetylation are expected to have weaker fluorescence.

To conclusively test the state of acetylation, WT ESAT-6 purified from *E. coli,* WT ESAT-6 purified from *M. smegmatis*, T2A, and T2S proteins were tested using mass spectrometry. As evidenced from previous studies, acetylation results in a mass increase of 42Da. Furthermore, trypsin and pepsin digestions of each protein were performed and analyzed for acetylation.

2.2.3 Determine the Effects of Acetylation on ESAT-6/CFP-10 Dissociation.

Given that the heterodimer complex purified from *E. coli* does not contain membrane lytic ability, we hypothesize that the ESAT-6 purified from *E. coli* does not have N-α-acetylation, thus it is not dissociated from CFP-10 at low pH. Here, the heterodimer purified from *M. smegmatis* will be dissociated by guanidine and tested for membrane lytic ability. It is expected that the newly separated proteins, including the mutated proteins, will maintain their membrane lysing activity. The proteins have been found to bind after incubation, (de Leon, 2012). Here the difference in binding efficiency of ESAT-6 purified from *M. smegmatis* will be compared to ESAT-6 purified from *E. coli* by using a native gel as previously described. Lastly, to determine the effect of acetylation on the dissociation of the heterodimer complex, surface plasmon resonance will be used to test

the binding affinity between ESAT-6 (WT and mutant) and CFP-10 using the methods as previously described (Rotherham, L. S., 2012). Briefly, CFP-10 will be fixed to a CM5 sensor-chip as the ligand, while ESAT-6 will be passed as analyte. We expect the non-acetylated ESAT-6 mutants to have higher binding affinity than acetylated ESAT-6.

Chapter 3 Experimental Approach

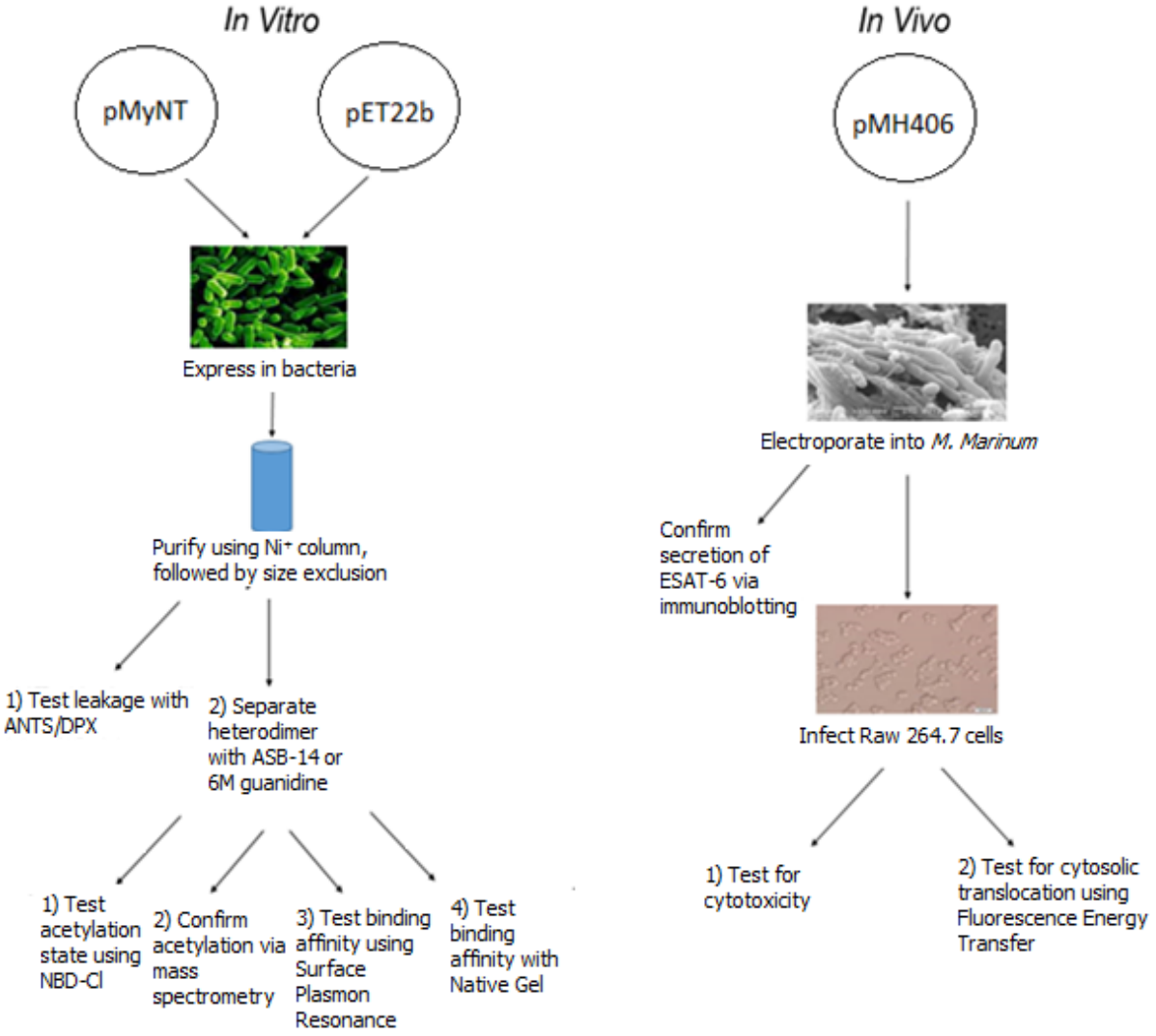

Figure 2: General Schematic of Methods: Project consisted of 2 major parts an *in vitro* and an *in vivo* portion. For *in vitro* experiments, two plasmids containing mutations T2A, T2Q, T2R and T2S were generated. Each plasmid was expressed and purified using a Ni^+ affinity chromatography followed by size exclusion. Resultant proteins were tested via ANTS/DPX leakage. Heterodimer proteins were separated via a minimum 3M guanidine and used to test acetylation state via NBD-Cl or mass spectrometry, or to test binding affinity via native gel or surface plasmon resonance. *In vivo* experiments consisted of generation of the four mutations in ESAT-6 and expressing this gene into *M. marinum.* Resultant strains was used to infect Raw 264.7 cells to test for cytotoxicity and cytosolic translocation. Immunoblotting was used to check for secretion of ESAT-6.

3.1 Preparation of Plasmids

The mutated ESAT-6 was prepared in three different plasmids, pET22b for expression in *E. coli*, pMyNT for expression in *M. smegmatis* and pMH406 for expression in *M. marinum*.

For pET22b plasmid, the appropriate primers were used to amplify the DNA via PCR (Table 3.1). Following PCR, samples were run on a 1 % agarose gel, and the appropriate band was excised and extracted using a QIAGEN gel extraction procedure. A double digestion was performed using NDE I and XHO I restriction enzymes, the products were loaded onto a 1% agarose gel and once again extracted using a QIAGEN gel extraction protocol. The digested inserts and vector were ligated using T4 DNA ligase. Following ligation, the plasmids were transformed into DH5α competent cells, and extracted via a Promega mini-prep procedure.

Mutated ESAT-6 was generated in pMH406 through site directed mutagenesis with a QuikChange II procedure from Agilent. Briefly, primers were designed to include the desired mutation at T2 of ESAT-6 (Table 3.1) and were used to amplify the DNA via PCR. Following PCR, the product were digested using Dpn-1 restriction enzyme to remove methylated DNA. Following digestion the products were transformed into XL-1 blue super-competent cells and extracted via a Promega mini-prep procedure.

Mutations in the pMyNT plasmid were generated via an overlap PCR procedure. Briefly, a F-primer was designed from N-terminal CFP-10 through the desired T2 mutation ESAT-6 as R-primer, while an additional set of primers, starting with a F-primer on the desired T2 mutation and ending at the C-terminus of ESAT-6 were generated to yield two fragments (one from N-terminal CFP-10 to mutation(NM), another from mutation to C-

terminal ESAT-6 (MC)) (Table 3.1). Both of these fragments were then used as template and amplified using the primer from N-terminal CFP-10 and C-terminal ESAT-6 to yield a completed fragment with the mutation in between. After amplification, the fragments were run in a 1% agarose gel, excised, and then purified via a QIAGEN gel extraction method. The NM and MC fragments were then used as templates, and primers from N-terminal CFP-10 and C-terminal ESAT-6 were used to amplify the completed PCR product. The completed insert was then double digested using BAMHI and NCOI. Digested inserts and vectors were ligated using T4 DNA ligase and transformed into DH5α competent cells

Table 1: Primers Used for Cloning. All the primers used for cloning are listed here. PMyNT used overlap PCR, meaning two fragments were created separately, then combined by using both fragments as a template and Forward Primer from fragment 1 and Reverse Primer from fragment 2.

Vector and Mutation	F-Primer Sequence	R-Primer Sequence
pET22b-T2A	5'-AAGGATCCATGGCAGAGCAGCAGTGGAATTC-3'	5'-TGGTGGTGGTGGTGGTGTGCGAACATCCCAGTG-3'
pET22b-T2Q	5'-AAGGATCCATGCAAGAGCAGCAGTGGAATTC-3'	5'-TGGTGGTGGTGGTGGTGTGCGAACATCCCAGTG-3'
pET22b-T2R	5'-AAGGATCCATGAGAGAGCAGCAGTGGAATTC-3'	5'-TGGTGGTGGTGGTGGTGTGCGAACATCCCAGTG-3'
pET22b-T2S	5'-AAGGATCCATGAGTGAGCAGCAGTGGAATTC-3'	5'-TGGTGGTGGTGGTGGTGTGCGAACATCCCAGTG-3'
pMyNT -T2A	Fragment 1: 5'-GCCATGGCAGAGATATGGCAGAGATGAAGA-3' Fragment 2: 5'-GAAACGGAGCAAAAACATGGCAGAGCAGCAGTGGAATTTC-3'	Fragment 1: 5'-GAAATTCCACTGCTGCTCTGCCATGTTTTTGCTCCGTTTC-3' Fragment 2: 5'-TAGCGATATCGAATTCGGATCCTTATGCGAA-3'
pMyNT -T2Q	Fragment 1: 5'-GCCATGGCAGAGATATGGCAGAGATGAAGA-3' Fragment 2: 5'-GAAACGGAGCAAAAACATGCAAGAGCAGCAGTGGAATTTC-3'	Fragment 1: 5'-GAAATTCCACTGCTGCTCTTGCATGTTTTTGCTCCGTTTC-3' Fragment 2: 5'-TAGCGATATCGAATTCGGATCCTTATGCGAA-3'
pMyNT -T2R	Fragment 1: 5'-GCCATGGCAGAGATATGGCAGAGATGAAGA-3' Fragment 2: 5'-GAAACGGAGCAAAAACATGAGAGAGCAGCAGTGGAATTTC-3'	Fragment 1: 5'-GAAATTCCACTGCTGCTCTCTCATGTTTTTGCTCCGTTTC-3' Fragment 2: 5'-TAGCGATATCGAATTCGGATCCTTATGCGAA-3'
pMyNT -T2S	Fragment 1: 5'-GCCATGGCAGAGATATGGCAGAGATGAAGA-3' Fragment 2: 5'-GAAACGGAGCAAAAACATGAGTGAGCAGCAGTGGAATTTC-3'	Fragment 1: 5'-GAAATTCCACTGCTGCTCACTCATGTTTTTGCTCCGTTTC-3' Fragment 2: 5'-TAGCGATATCGAATTCGGATCCTTATGCGAA-3'
Pmh406 -T2A	5'-GAAACGGAGCAAAAACATGGCAGAGCAGCAGTGGAATTTC-3'	5'-GAAATTCCACTGCTGCTCTGCCATGTTTTTGCTCCGTTTC-3'
Pmh406 -T2Q	5'-GAAACGGAGCAAAAACATGCAAGAGCAGCAGTGGAATTTC-3'	5'-GAAATTCCACTGCTGCTCTTGCATGTTTTTGCTCCGTTTC-3'
Pmh406 -T2R	5'-GAAACGGAGCAAAAACATGAGAGAGCAGCAGTGGAATTTC-3'	5'-GAAATTCCACTGCTGCTCTCTCATGTTTTTGCTCCGTTTC-3'
Pmh406 -T2S	5'-GAAACGGAGCAAAAACATGAGTGAGCAGCAGTGGAATTTC-3'	5'-GAAATTCCACTGCTGCTCACTCATGTTTTTGCTCCGTTTC-3'

3.2 Expression and Purification of Proteins

The pET22b plasmids containing target genes were transformed into BL21 (DE3)-C41 competent cells. A single colony was picked and grown overnight in 30ml of Luria-Bertani broth (LB) as a start-up culture at 37°C while shaking at 250 RPM. Next, 5ml of

the start-up culture was used to inoculate 1L of LB. The culture was then allowed to reach an OD_{600} of 0.6-0.8, at which point the culture was induced by adding Isopropyl β-D-1-thiogalactopyranoside (IPTG) to a final 1mM concentration; the culture was incubated for a further 3-8 hours post induction. Proteins were purified by an on-column refolding protocol, as previously mentioned (de Leon, 2007), using a Ni^{+} affinity column. The protein resulting from the Ni^{+} elution is concentrated using a 3000 MWCO viva spin and injected into a Superdex-75 size exclusion column for size exclusion chromatography.

Genes in pMyNT plasmid were electroporated into *M. smegmatis*. A single colony was picked and allowed to culture for ~2 days at 37°C while shaking at 250 RPM in 7h9 medium supplemented with OADC as a start-up culture. Approximately, 10 ml of start-up culture was used to inoculate 1L of 7H9 media supplemented with glucose ($0.2\%_{(w/v)}$), glycerol ($0.2\%_{(v/v)}$), and tween-80($0.05\%_{(v/v)}$). The 1L culture was incubated overnight or until it reached an OD_{600} of 2.0. The culture was induced using 2g acetamide and allowed to culture for 1 day. The protein is typically soluble and is purified by sonicating with protease inhibitor cocktails. The sonicated sample was centrifuged at 15000RPM for 40 minutes. The supernatant was loaded onto a Ni^{+} affinity column. The purified protein was concentrated using a 5000 MWCO viva spin to final 1ml volume. The concentrated sample was injected into a Superdex-75 column for a size exclusion chromatography.

3.3 Generation of *M. marinum strains*

M. marinum KO strain was electroporated using the pMH406 plasmids. The plasmid was electroporated at a voltage of 2500 U, capacitance of 25 µF, resistance of 1000 Ω. The sample was incubated in 10ml of 7h9 medium for 4 hours at 30°C. The

sample was centrifuged and re-suspended into 1ml for plating. The plates were incubated for 2 weeks at 30°C in darkness.

3.4 Growth Conditions for RAW 264.7 Cells

Raw 264.7 cells were used for infection. They were cultured in DMEM medium containing 10% fetal bovine serum (FBS) with penicillin and streptomycin. The cells were grown at 37°C with 5% CO_2.

3.5 Separation of Heterodimer with ASB-14 or 6M Guanidine.

The CFP-10 and ESAT-6 heterodimer complex can be separated via incubation with ASB-14 at 1X critical micelle concentration (8mM ASB-14) or 6M guanidine for 1 hour or overnight, respectively, in 4°C. Following incubation, the proteins were purified using a Ni^{+} affinity column. CFP-10 contains a hexa-histidine tag, while ESAT-6 does not meaning that flow-through collected contains ESAT-6, while the elution sample consists of CFP-10. If the sample is separated using ASB-14, it is diluted to lower the critical micelle concentration of ASB-14 making the detergent weaker and easier to remove via a thermos scientific detergent removal kit. Following the detergent removal kit, an acetone precipitation was used to remove residual detergent. Leftover acetone was evaporated and the sample was re-suspended in 1ml of a 25mM NaH2PO4 and 100mM NaCl buffer. If the sample is separated under denaturing conditions with 6M guanidine, ESAT-6 and CFP-10 will be concentrated using a 3000 MWCO or 5000 MWCO viva spin, respectively into a 1ml sample. The concentrated 1ml sample from either source can be injected into a Superdex-75 column for further purification and buffer exchange.

3.6 Liposome Leakage Assay

Liposomes were prepared as previously described (Jacquez, 2012). Briefly, 1,2-dioleoyl-*sn*-glycero-3-phosphocholine and 1,2-dioleoyl-*sn*-glycero-3-[(N-(5-amino-1-carboxypentyl)iminodiacetic acid)succinyl] (nickel salt) were mixed at appropriate ratios, dried using nitrogen gas, and then placed under a vacuum overnight. The samples were rehydrated and added 8-aminonapthalene-1,3,6 trisulfonic acid (ANTS)/p-xylene-bis-pyridinium bromide (DPX). Suspended liposomes were submitted through 6 freeze/thaw cycles using ethanol with dry ice and hot water, respectively. The lipids were extruded through a 0.2 µm membrane 20 times to form the liposomes. As the liposomes are formed, high concentrations of ANTS and DPX will be entrapped inside liposomes, where the ANTS fluorescence will be quenched by DPX. The liposomes were desalted using a hitrap desalting column. Upon pore formation, ANTS and/or DPX will be released out of the liposomes, resulting in de-quenching of ANTS fluorescence. The exhibited measurable fluorescence was quantified in an ISS K2 phase modulation fluorometer.

3.7 Measuring Macrophage Cell Death Using the Cytotoxicity Assay.

Raw 264.7 macrophages were plated in 24 well plate at a concentration of $5X10^5$ for infection the following day. After growing a viable culture of *M. marinum,* the bacteria was prepared via a single cell preparation protocol, as previously described (Takaki, K., 2013), to break up the cells which have a high tendency to form cellular clumps. Briefly, the cells were washed with PBS and broken up using a high gauge needle. The cells were centrifuged lightly and optical density OD_{600} was measured to determine bacterial concentration. The *M. marinum* after single cell preparation was used to infect the Raw 264.7 macrophages at a multiplicity of infection (MOI) of 10 for 1 hour. Following the infection the macrophages were washed 3 times to remove bacteria and incubated for 3

hours. The macrophages were stained using calcein-AM and ethidium homodimer for 30 minutes, enabling visualization under a fluorescent microscope for green (live) and red (dead) cells. The number of dead cells were quantified and compared throughout all the strains.

3.8 Fluorescence Resonance Energy Transfer

Raw 264.7 macrophages were plated in 6 well plates at a concentration of $2.5X10^6$ cells. *M. marinum* cultures were prepared using the previously described single cell preparation technique in section 4.7. Cells were infected at an MOI of 10 for 2 hours. Following infection, macrophages were washed 3 times using PBS. DMEM media with 10% FBS was added to the cells and incubated for ~2 days. The samples were then excited at 409nm and emissions measured at 450nm and 535nm. The study works by observing a change from 535nm (green) to 450nm (blue) as a result of a reaction between the chemical probe and β-lactamase, as the bacteria escapes the phagosome it is enclosed in, the β-lactamase expressed on the cell wall of the bacteria reacts with the chemical probe causing a shift from green to blue fluorescence. The fluorescence was compared as a ratio, with a higher blue/green ratio indicating a greater shift of bacteria from phagosome into cytosolic space.

3.9 Western Blotting

The secretion and expression of ESAT-6 was measured using Western blotting. *M. marinum* cultures were grown in 7h9 to mid-log phase. They were then washed with PBS and passaged to Sauton's media while normalizing all cultures to OD_{600} of 0.8. They were allowed to grow for two days until harvest. The cultures were centrifuged and the

supernatant was used to detect secretion of ESAT-6, while the pellet was used to detect expression of ESAT-6 within the cells. Supernatant of ESAT-6 culture was prepared by concentrating using a 5000mwco viva spin at least 75x. The resulting culture was then concentrated using a trichloroacetic acid precipitation. Cell lysate was resuspended in 1ml of PBS + protease inhibitor cocktail and sonicated at 30% amplitude pulsing for 30 seconds and resting for 1 minute 5 times.

3.10 NBD-Cl

NBD-Cl was used to determine the acetylation state of the different types of ESAT-6 protein. A 1ml sample containing 6µM of proteins with 0.5mM NBD-Cl wias incubated for 1 hour at room temperature. The samples were excited at 460nm and the emissions at 535nm were recorded. The samples were measured within a period of 24 hours with different intervals in between.

3.11 Mass Spectrometry

Acetylation will be confirmed via mass spectrometry. Here, the ESAT-6 protein from *M. smegmatis* were tested to see if the acetylation or an increase of 42 Da is seen as compared to WT ESAT-6 purified from *E. coli*, furthermore, T2S and T2A mutants purified from *M. smegmatis* were also tested. The four purified proteins were analyzed by 2hr-1d-LC-MS/MS on QEClassic. For more reliable data, the four purified proteins were digested via FASP-trypsin and pepsin. All peptide mixtures were analyzed by 2hr-1d-LC-MS/MS on QEClassic. Following a PD2.1 search against a combined database containing *E. coli* BL21 and *M. smegmatis* M1552 and other common contaminants was performed.

3.12 Native Gel

The binding efficiency to CFP-10 from ESAT-6 purifed from *E. coli* was compared to ESAT-6 purified from *M. smegmatis* via native gel electrophoresis. ESAT-6 from both sources was incubated with CFP-10 at different molar ratios (0.5x, 1.0X, 1.5X, and 2.0X), for 2 hours at room temperature. The samples were loaded onto a native gel to observe for efficiency at which the proteins from a complex and for ability of ESAT-6 to deplete CFP-10.

3.13 Surface Plasmon Resonance

The binding affinity of ESAT-6 was tested by using surface plasmon resonance. CFP-10 was bound to a CM5-sensor chip via amine coupling. N-hydroxysuccinimide, and N-ethyl-N'-(3-dimethylaminopropyl carbodiimide hydrochloride will be injected. CFP-10 at 200nM was injected at 5µl/minute followed by ethanolamine-HCl. ESAT-6 purified from *E. coli* was passed through the sensor-chip at equimolar concentration as CFP-10. Following this experiment ESAT-6 purified from *M. smegmatis* was passed through the sensor-chip, to which CFP-10 was attached. The binding affinity of the two proteins was compared.

Chapter 4: Results

4.1 Mutated ESAT-6 Was Generated and Proteins Were Purified

Following PCR, the mutations T2/A, T2/Q, T2/R, T2/S at ESAT-6 were achieved as shown on figure 3. Mutated ESAT-6 was generated in pET22b for expression of ESAT-6 in *E. coli*, pMyNT for expression of CFP-10 and ESAT-6 as a heterodimer in *M. smegmatis*, and pMH406 for complementation with the ESAT-6 gene into a KO *M. marinum* strain.

```
ESAT-6        MTEQQWNFAGIEAAASAI
ESAT-6:T2S    MSEQQWNFAGIEAAASAI
ESAT-6:T2Q    MQEQQWNFAGIEAAASAI
ESAT-6:T2R    MREQQWNFAGIEAAASAI
ESAT-6:T2A    MAEQQWNFAGIEAAASAI
              *  ****************
```

Figure 3: Mutations generated in ESAT-6: Threonine 2 was mutated to either A, Q, R or S. Mutations were created for lone ESAT-6, Complexed ESAT-6 or in ESAT-6 for complementation into *M. marinum*.

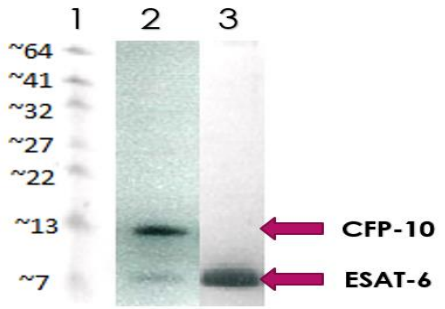

Figure 4: Different Fractions for purified ESAT-6 complexed with CFP-10 or lone ESAT-6: Typical fractions for any protein heterodimer (2) or lone ESAT-6 (3).

Following generation of plasmids, proteins were purified using an on-column refolding protocol for unsoluble ESAT-6 and standard Ni^{+} affinity for the soluble heterodimer. Proteins from either source were further purified using size exclusion chromatography. All purified proteins were highly pure as evidenced by SDS-PAGE (Figure 4). Heterodimer protein generally consisted in nearly a 1:1 expression of CFP-10 to ESAT-6.

4.2 ANTS/DPX Assay Reveals T2Q, T2R and T2A Mutants Failed to Lyse Liposomes

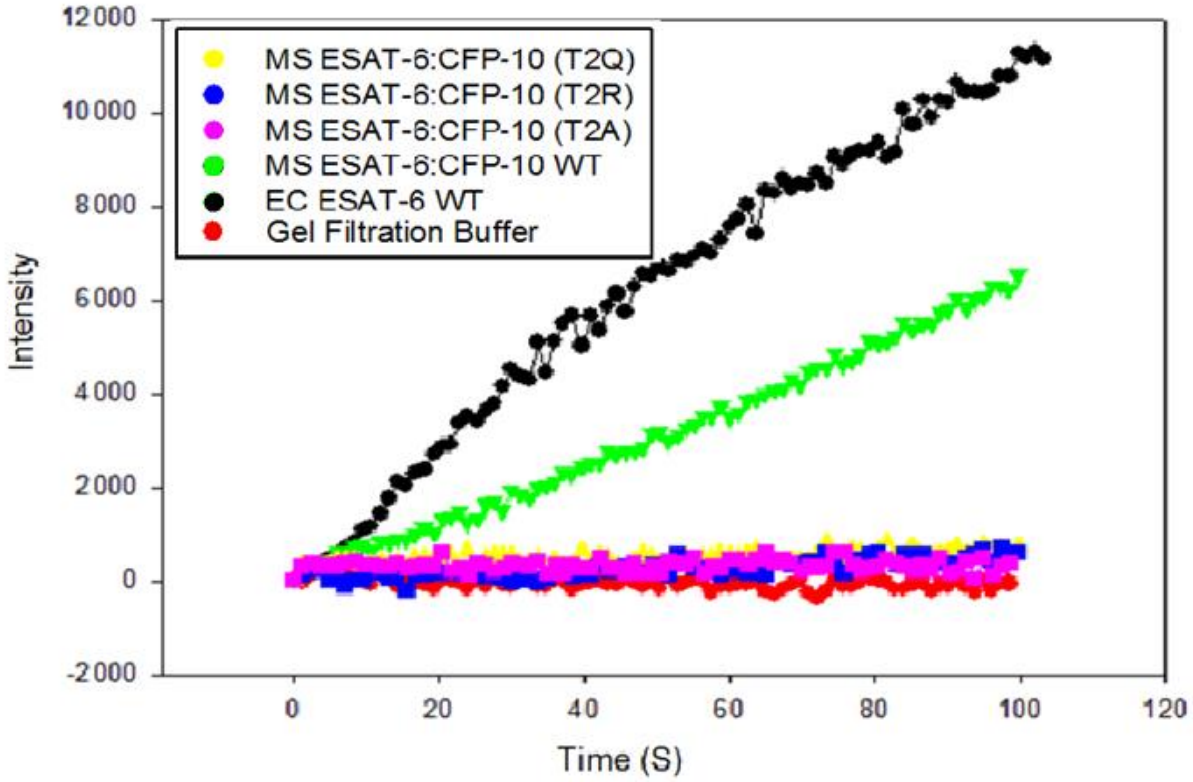

Figure 5: Liposome Leakage Assay of complexed ESAT-6: WT ESAT-6 purified from *E.* coli was used as a positive control for membrane lysing activity. WT heterodimer ESAT-6 showed less activity that WT ESAT-6. None of the mutations successfully induced liposome membrane lysis.

Results indicate the ESAT-6 mutants complexed with CFP-10, were unable to induce the same membrane lysing ability as ESAT-6 alone. The activity of complexed ESAT-6 and CFP-10 was approximately half of the intensity that lone ESAT-6 had (Figure 5). A possible explanation could be that the ESAT-6 and CFP-10 complex was not dissociated completely, thus not having the same activity wild-type ESAT-6. The mutants containing T2Q, T2R or T2A mutations of ESAT-6 failed to induce fluorescence, indicating that the

proteins were incapable of lysing the membrane of the liposomes. To confirm that ESAT-6 activity was not hindered by the mutations, ESAT-6 proteins containing each of the mutations were purified from *E. coli* and compared to WT ESAT-6 (Figure 6). These ESAT-6 mutated proteins showed similar membrane-lysing activity as WT ESAT-6 highlighting that the mutations themselves did not affect the activity of ESAT-6. Both figures indicate the importance of ESAT-6 and CFP-10 interaction. When complexed activity of ESAT-6 is not possible, all mutants were incapable of lysing liposomal membranes. However, ESAT-6 purified alone confirmed the activity of ESAT-6 was unaffected by the mutations. Data suggests the separation of ESAT-6 from CFP-10 was hindered as a result of the mutations, explaining why complexed ESAT-6 with mutations failed to induce membrane lysis.

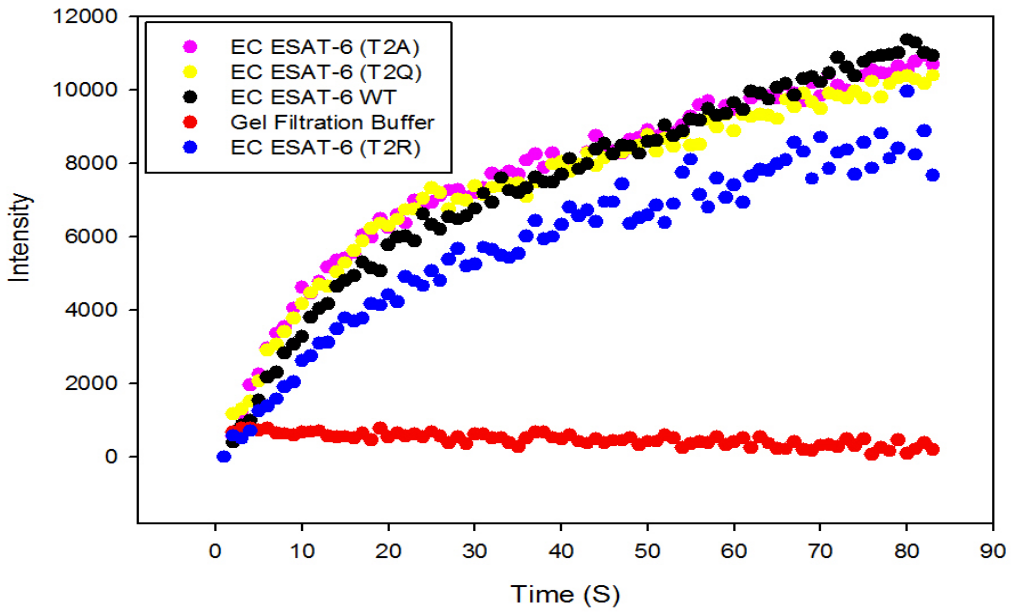

Figure 6 ESAT-6 activity remains despite mutations: ESAT-6 purified by itself showed similar activity regardless of mutations.

4.3 Secretion of ESAT-6 was Revealed Using Western Blot

Secretion of ESAT-6 after complementation of *M. marinum* with either WT or mutated species was confirmed via immunoblotting. ESAT-6 was detected in both culture filtrate (CF) and cell lysate (CL) for all strains with the exception of KO as expected (Figure 7). Blotting against the AG85 complex was used as a loading control for this experiment given that the complex is a secreted protein, which was detected in both CL and CF of all generated strains. As a control for secretion GroEL, a protein found only as an integral cell membrane protein, was blotted against. As expected none was found in CF but was clearly observed in CL samples. This assay served as a control for *in vivo* experiments. Detection of ESAT-6 in both CL and CF confirmed the protein's expression and release was not hindered by the mutations.

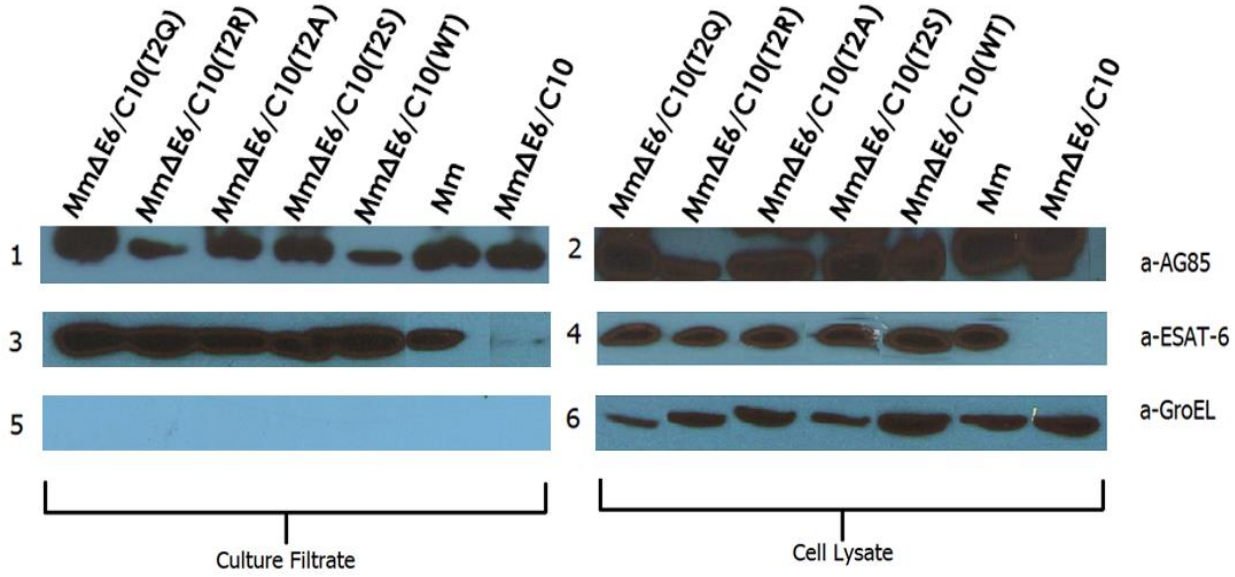

Figure 7: ESAT-6 is being secreted: ESAT-6 secretion and expression is unaffected by mutations (3,4). AG85 was used as a positive control for protein secretion and expression (1,2), while GroEL was used to control for secretion (5,6).

4.4 Mutated ESAT-6 Had Less Impact on Raw 264.7 Macrophages

Cytotoxicity studies revealed, *in vivo,* the detrimental effects of a mutated ESAT-6. *M.* marinum complemented with ESAT-6 containing T2Q, T2R, or T2A mutations caused minimal cell death compared to the Wild-Type *M marinum* or strains complement with WT-ESAT-6 or T2S mutation in ESAT-6 (Figure 8). The macrophages infected with the KO strain as well as PBS, which served as a negative and vehicle control, respectively, caused negligible cell death indicating there were no additional factors affecting cell death. The strain complemented with WT ESAT-6 showed similar activity to the WT *M. marinum* strain demonstrating that electroporation of the WT ESAT-6 gene could restore activity akin to WT rather than intermediately as the T2Q, T2R, and T2A mutants. The T2S mutant showed similar activity as did the WT, indicating that a residue with similar biochemical properties retains similar function.

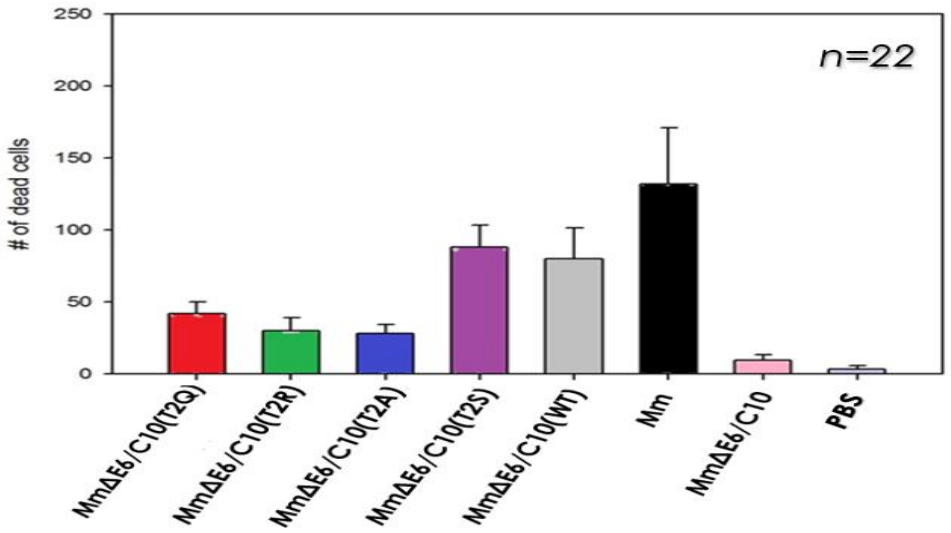

Figure 8: Differential Cytotoxicity of *M. marinum* strains: Mutated ESAT-6 showed defected infection. WT, complemented strain (MmΔE6/C10(WT)) and T2/S (MmΔE6/C10(T2S)) mutant retained significantly higher activity than did T/2Q(MmΔE6/C10(T2Q)), T2/R (MmΔE6/C10(T2R)) and T2/A (MmΔE6/C10(T2A)) mutants.

4.5 Fluorescence Resonance Energy Transfer Revealed Mutated ESAT-6 Had Significantly Lower Cytosolic Translocation

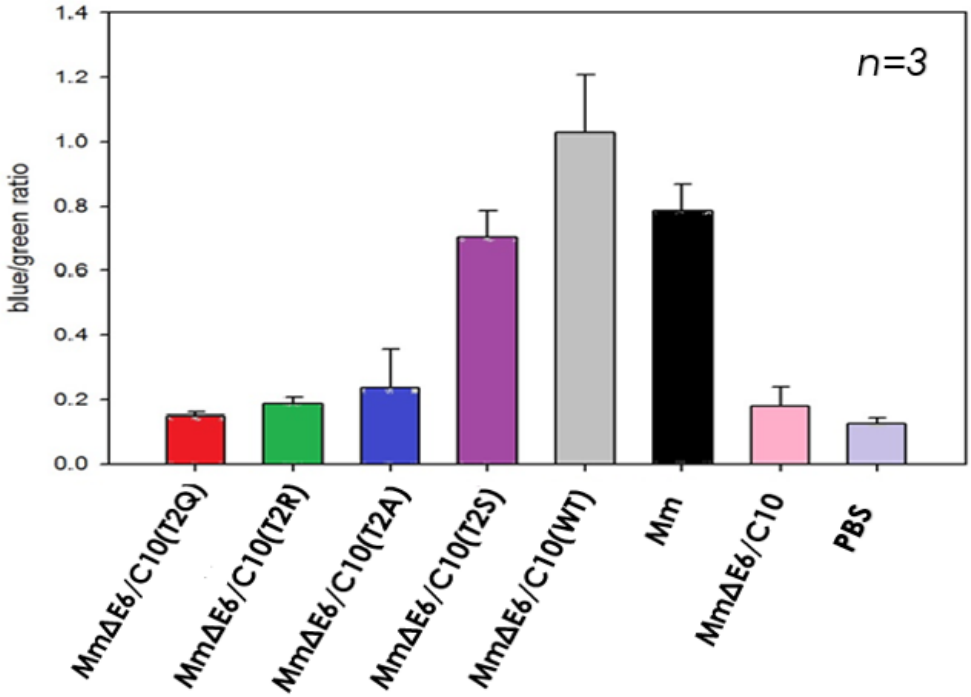

Figure 9: Fluorescence Resonance Energy Transfer: The different mutations had negligible blue/green ratio indicating small amounts of cytosolic translocation. However, the noticed translocation may be greatly reduced, a negative control containing only PBS showed similar ratios. Undoubtedly, S mutant complemented KO strain with WT ESAT-6, and WT *M. marinum* strain all showed a higher blue/green ratio.

As shown by fluorescence resonance energy transfer, the T2Q, T2R, T2A mutants had a significantly lower intensity than did T2S, WT *M.* marinum and WT ESAT-6 complemented KO strains. Once more, the KO and negative control had negligible shift in blue/green ratio (Figure 8). Interestingly, the blue/green ratio from T2Q, T2R and T2A was nearly the same as KO and negative control. This data suggests a small portion of the blue/green shift observed in the T2/Q, T2/R, or T2/A mutants may be due to other factors, rather than the activity of the strains themselves. The T2/S strain, WT *M. marinum* and KO complemented with WT ESAT-6 showed significantly higher blue/green ratio.

Since the acetylation negative strains are presumed to have no or severely defected membrane lytic activity, the results here are consistent with what was previously observed, the mutants are unable to translocate into the cytosol as opposed to the active strains.

4.6 Successful Separation of Heterodimer was Achieved using ASB-14 or 6M Guanidine

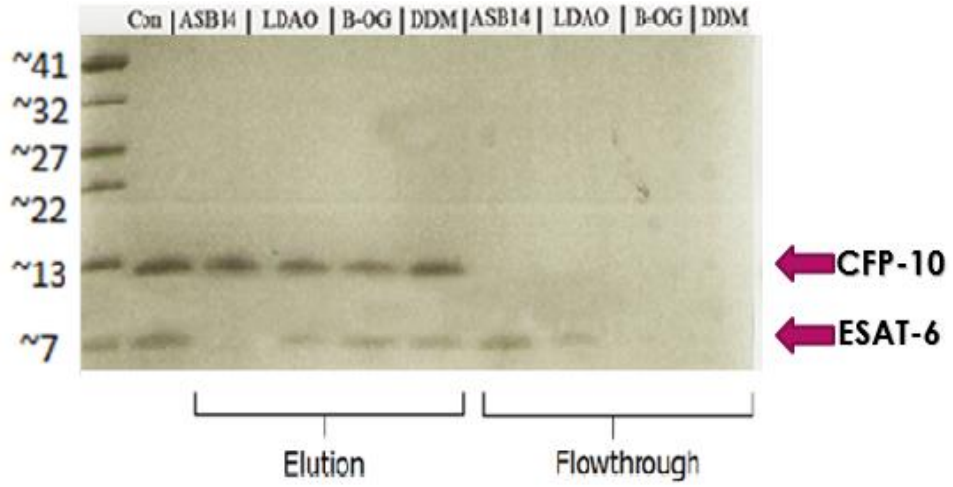

Figure 10 ASB-14 successfully separates ESAT-6/CFP-10 heterodimer: Use of multiple detergents revealed zwitterionic detergents to be the most effective at disrupting ESAT-6/CFP-10 interaction as observed by ASB-14 and LDAO. All samples were tested at 1X critical micelle concentration.

Treatment with detergents revealed that high concentration of detergents used will disrupt interaction between ESAT-6 and CFP-10 allowing for separation of the heterodimer complex. Incubation with ASB-14, LDAO, B-OG, or DDM at 10X critical micelle concentration will separate the heterodimer (data not shown). Incubation with detergents at 1X CMC revealed a stronger disruption of the heterodimer with ASB-14. LDAO, another zwitterionic detergent appears to also cause separation of the

heterodimer at 1X CMC, but still to a lesser extent than ASB-14. Following incubation with detergents, the samples were run through a Ni+ affinity chromatography to separate ESAT-6 which lacks a his-tag from CFP-10. Flow-through sample consisted of ESAT-6 that was washed out as unbound sample, while elution sample consisted of CFP-10 (Figure 10). Following separation of the proteins, extensive detergent removal was performed.

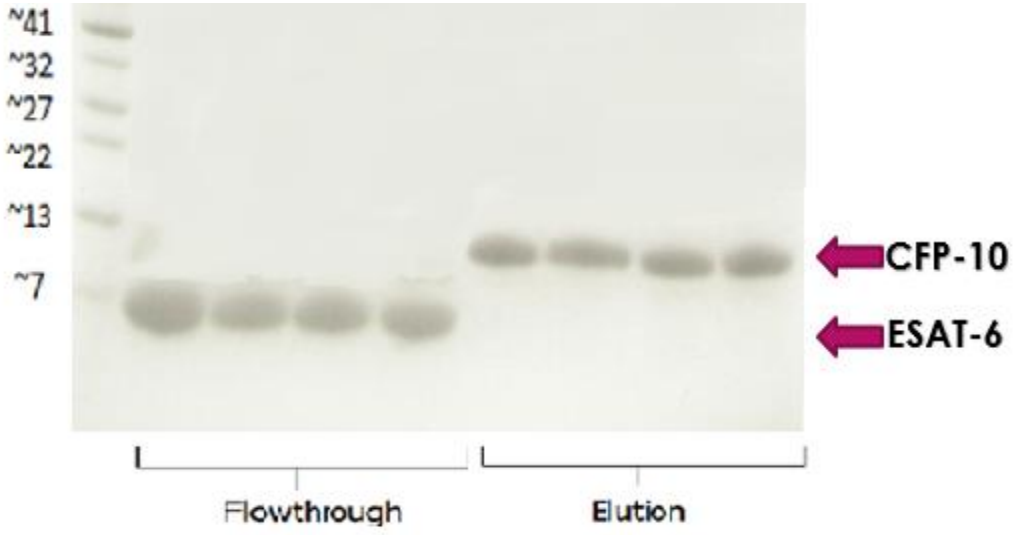

Figure 11: 6M guanidine treatment separates ESAT-6/CFP-10 heterodimer: ESAT-6 and CFP-10 interaction was disrupted by 6M guanidine, flowthrough samples consisted of ESAT-6, devoid of any CFP-10.

Treatment using 6M guanidine successfully separated the heterodimer complex. Following an overnight incubation with 6M guanidine samples were purified using a Ni+ affinity chromatography. Once more unbound samples represented ESAT-6 while elution samples consisted of CFP-10. Samples were dialyzed using tris-buffered saline to remove excess urea or were submitted to buffer exchange chromatography

using a superdex 75 column. Separation and recovery of proteins was observed via SDS-PAGE (Figure 11).

4.7 NBD-Cl Revealed Lack of Acetylation for Mutated ESAT-6; Confirmed Acetylated ESAT-6 from *M. smegmatis*

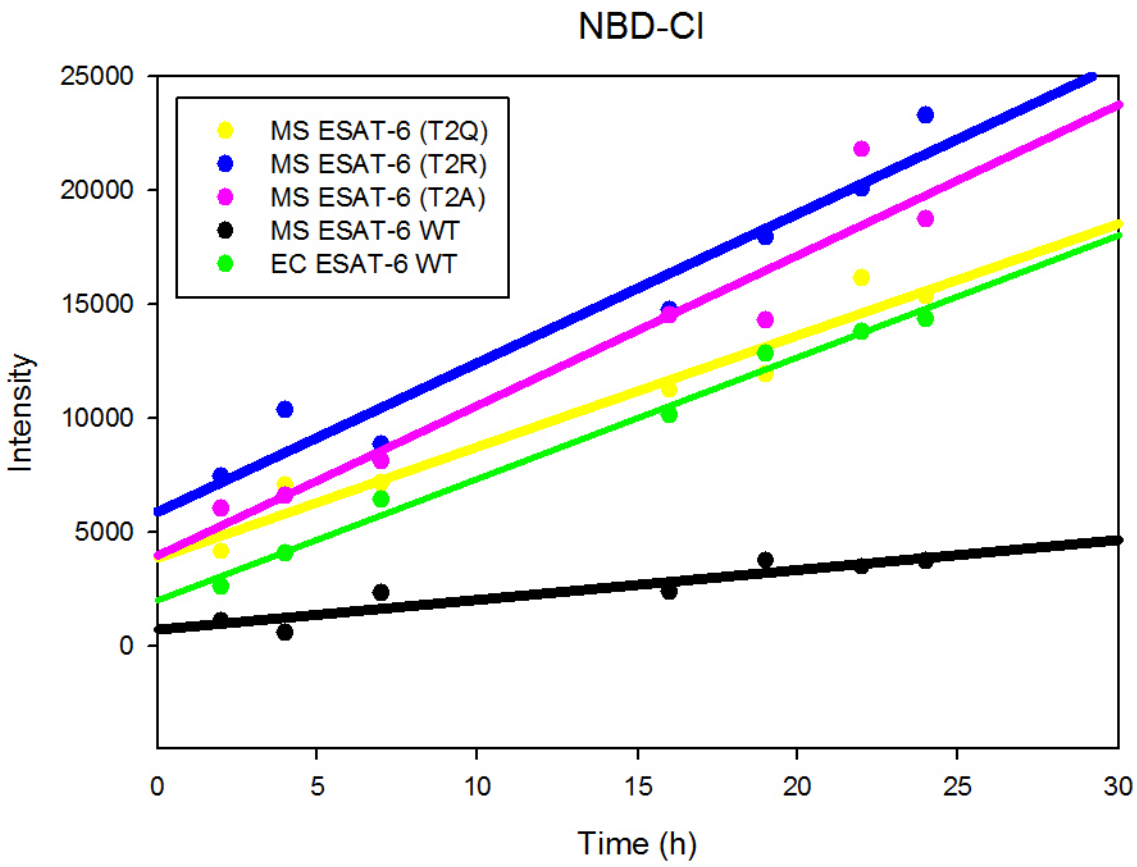

Figure 12: Mutated ESAT-6 contains Free N-terminal site: Evidence of differential N-terminal acetylation was observed. As suspected, protein free of N-terminal acetylation showed higher fluorescence indicating a free N-terminal site. ESAT-6 purified from *M. smegmatis* showed a much lower signal implying a blocked N-terminal site presumably by an acetyl group.

The heterodimer complex was incubated with ASB-14 to disassociate the complex. The resulting ESAT-6 proteins were tested using using 4-chloro-7-nitrobenzofurazan

(NBD-Cl), a fluorophore that binds at the N-α-terminal site of a protein, and emits fluorescence after binding. Proteins with an acetyl group have a blocked binding site for NBD-Cl, which will not allow the fluorophore to bind and emit fluorescence. This study revealed more intense fluorescence on ESAT-6 purified from *E. coli* and the mutants purified from *M. smegmatis* than WT ESAT-6 from *M. smegmatis*. The T2Q, T2R, and T2A mutants had similar intensity to ESAT-6 from *E. coli*, indicating the lack of acetylation. The ESAT-6 protein from *M. smegmatis* had less intensity than the other types of ESAT-6 indicating it to be acetylated (Figure 12). Furthermore, incubation period of 24 hours significantly increased intensity on other proteins while rise in intensity for presumably acetylated ESAT-6 was nonexistent.

4.8 Mass Spectrometry Distinguishes N-α-terminally Acetylated VS. Un-Acetylated Proteins

Intact protein analysis revealed a methionine loss with acetylation for WT ESAT-6 from *M. smegmatis* representing over 95% of abundant species. T2S mutant revealed

similar results with the acetylated protein representing about 80% of abundant species. WT ESAT-6 from *E. coli* showed acetylation without a methione loss representing ~40% of abundant species, lastly T2A showed intact species with a methionine loss representing 99% of abundant species (data not shown). For more conclusive results trypsin and pepsin digestions of proteins were performed. Resultant

peptides were analyzed via mass spec and a PD2.1 search was performed looking for all acetylation and oxidations of the proteins. Pepsin digestions showed results consistent with previous mass spec analyses; however, some samples did not have N-terminus recovery (Table 2). To supplement previous findings, trypsin digestion was performed and N-α-terminal acetylation for WT ESAT-6 and T2S from *M. smegmatis* was confirmed. WT ESAT-6 purified from *E. coli* did in fact reveal acetylation, but none was found at the N-terminus. Consistent with previous findings, methionine loss did not occur for ESAT-6 from *E. coli.* Lastly, as was expected T2A showed no signs of N-α-terminal acetylation (Table 3; Figure 13). Furthermore, oxidation of methionine is a common modification and

Protein Name	**Sequence Coverage**	**N-terminal Modification**	**Total Modifications**
Ms ESAT-6	99%	Met-loss; Acetyl-Thr	1 Acetyl; 2 Oxidation
EC ESAT-6	87%	N-terminus not recovered	2 Oxidation
Ms ESAT-6 (T2A)	63%	N-terminus not recovered	1 Oxidation
Ms ESAT-6 (T2S)	99%	Met-loss; Acetyl-Ser	1 Acetyl; 1 Oxidation

Table 2: Summary of mass spectrometry results following pepsin digestion: ESAT-6 from *M. smegmatis* and T2S mutated ESAT-6 show acetylation consistent with other findings. Other proteins did not have successful recovery of N-terminal sequence and cannot be assumed to lack acetylation.

Protein Name	Sequence Coverage	N-terminal Modification	Total Modifications
Ms ESAT-6	99%	Met-loss; Acetyl-Thr	4 Acetyl; 2 Oxidation
EC ESAT-6	100%	Oxidized-Meth	9 Acetyl; 3 Oxidation
Ms ESAT-6 (T2A)	99%	Met-loss	5 Acetyl; 2 Oxidation
Ms ESAT-6 (T2S)	99%	Met-loss; Acetyl-Ser	4 Acetyl; 2 Oxidation

Table 3: Summary of mass spectrometry results following trypsin digestion: Results here revealed an array of modifications to the resulting peptides. Over 90% of sequence recovery was obtained after analysis. ECE6 refers to ESAT-6 purified from *E. coli*, while MSE6 refers to ESAT-6 purified from *M. smegmatis.*

was helpful to indicate a conserved methionine in *E. coli* ESAT-6. The search after trypsin digestion also revealed other acetylations in different residues.

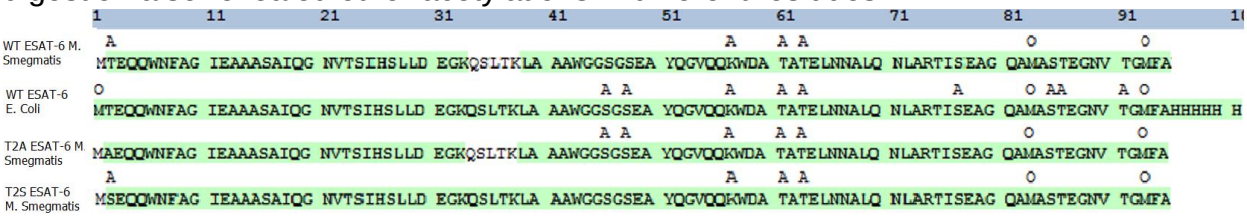

Figure 13: Sequence recovery of different ESAT-6 peptides from trypsin digestion: Here all modifications to the different types of ESAT-6 protein are denoted in their respective location. Acetylation is indicated by an "A" above the acetylated residue, while oxidations are denoted by an "O" above the affected residue. Green highlighting represents the sequence recovery.

4.9 Native Gel Reveals ESAT-6 From *E. coli* binds less efficiently than ESAT-6 from *M. smegmatis*

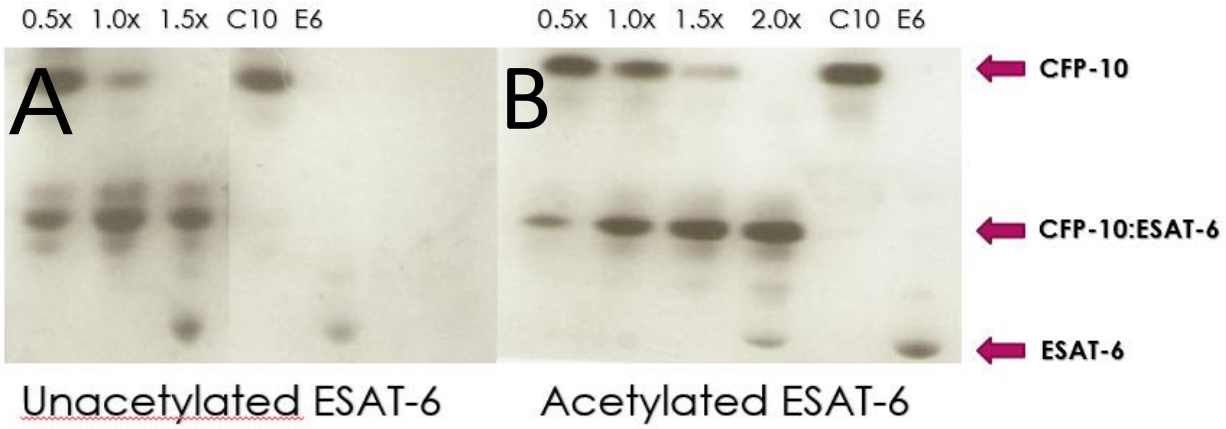

Figure 14: ESAT-6 from *M. smegmatis* is less prone to form a heterodimer: **(A)**Esat-6 purified from E. coli depleted CFP-10 at 1.5X molar ratio. **(B)** ESAT-6 purifed from M. smegmatis depleted ESAT-6 at 2.0X molar ratio.

Following incubation, ESAT-6 from *E. coli* depleted CFP-10 to form the heterodimer complex which migrated lower than CFP-10 but slightly above ESAT-6 (Figure 14A). ESAT-6 purified from *M. smegmatis* formed a complex with CFP-10 but failed to deplete CFP-10 at lower molar ratios (Figure 14B). The native gel in this study supports the theory that acetylation might hinder the binding affinity between CFP-10 and ESAT-6. A non-acetylated ESAT-6 from *E. coli* is able to associate more efficiently than an acetylated ESAT-6 from *M. smegmatis.*

4.10 Surface Plasmon Resonance Reveals Differential Binding Affinity of Acetylated Vs Un-acetylated ESAT-6

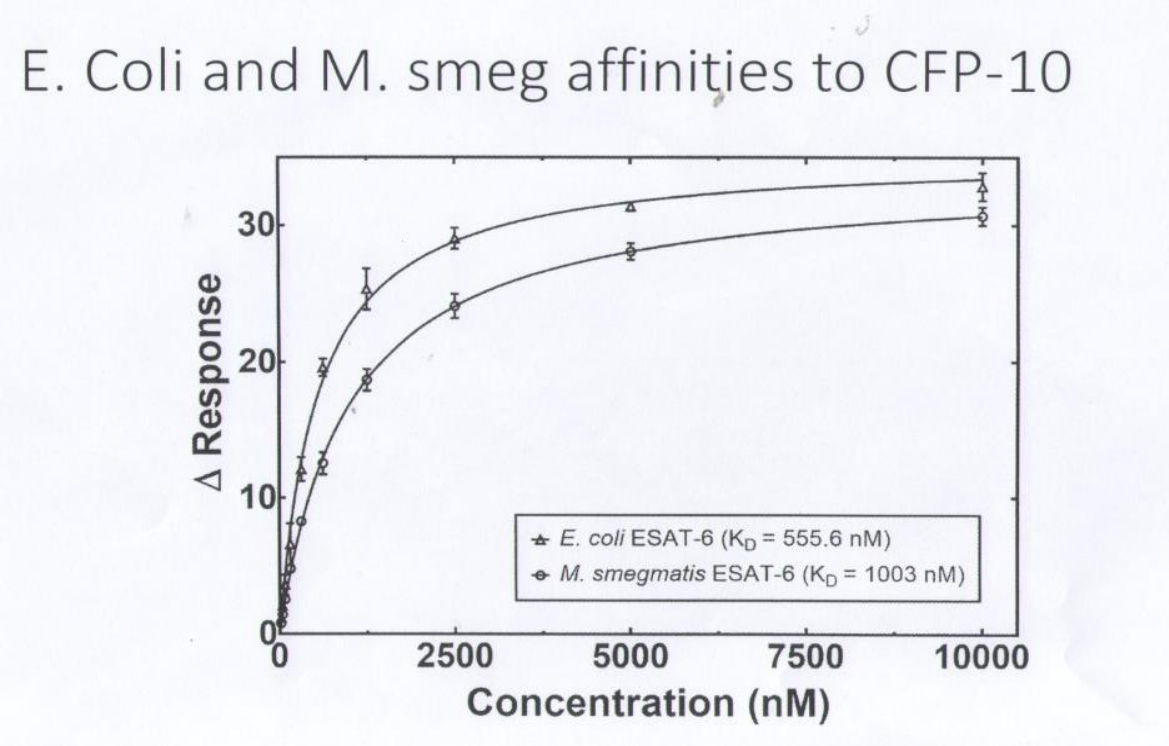

Figure 15 ESAT-6 from *M smegmatis* displays lower binding affinity than ESAT-6 from *E. coli:* Evidenced from surface plasmon resonance, ESAT-6 from *M. smegmatis* had a higher K_D than ESAT-6 from *E. coli*

CFP-10 was bound to a CM5 sensor chip using amine coupling. As evidenced from previous data, ESAT-6 from *M. smegmatis* contains acetylation at its N-terminus, while ESAT-6 from *E. coli* does not. Preliminary studies revealed the difference in binding affinity, as the un-acetylated ESAT-6 represented near double the binding affinity of an acetylated species.

Chapter 5 Discussion, Conclusion, Future Direction

5.1 Discussion

The experiments here reveal the importance of N-α-terminal acetylation in the pathogenesis of ESAT-6. Removal of the acetylation mechanism results in significantly reduced activity. The physiological importance of N-α-terminal acetylation can't be overstated for this reason. Results indicate that the ESAT-6 mutants, when complexed with CFP-10, were unable to induce the same membrane lysing ability as the wild type. When they were alone (without CFP-10), the ESAT-6 mutants showed significantly defected membrane-lysing activity, suggesting that the mutants inhibited the pH-dependent dissociation of ESAT-6 from CFP-10 without affecting the activity of ESAT-6 itself. Cytotoxicity studies revealed in vivo the detrimental effects of a mutated ESAT-6. The T2/Q, T2/R, and T2/A mutants caused diminutive cell death, compared to Wild-Type *M. marinum*, T2/S mutant, and KO strain complemented with WT ESAT-6. The additional T2/S mutant, showed similar activity than did the wild-type, indicating a residue with similar biochemical properties, did in fact retain similar function. FRET revealed the mutations T2/Q, T2/R, and T2/A resulted in less cytosolic translocation than Wild-Type *M. marinum*, T2/S mutant, and KO strain complemented with WT ESAT-6, reiterating the significance of N-α-terminal acetylation to *M. marinum*. The results clearly highlight the importance of threonine-2 and more importantly, the effect N-α-terminal acetylation has on the activity of ESAT-6. Just as importantly, western blotting confirmed the secretion of ESAT-6 indicating no other factors had been affected by the mutations. The attenuated virulence and lower cytosolic translocation highlights the physiological importance of N-α-terminal acetylation and differential liposome lysing ability between complexed and lone

ESAT-6, hints the mutations on the ESAT-6 protein render it incapable of efficient dissociation from its molecular chaperone.

Perhaps one of the more important aspects of this project was the separation of the heterodimer complex. Through this separation, further characterization of ESAT-6 was enabled, as a reliable method to isolate acetylated ESAT-6 was created. NBD-Cl testing demonstrated more fluorescence on ESAT-6 purified from *E. coli* and the mutants purified from *M. smegmatis* than the Wild-Type ESAT-6 from *M. smegmatis.* NBD-Cl will only show fluorescence when it binds to proteins at the site where N-α-terminal acetylation would take place. *E. coli* does not contain the exact same N-α-terminal acetyltransferases present in *M. smegmatis*, therefore ESAT-6 purified from *E. coli* should show more activity than ESAT-6 purified from *M. smegmatis*. The mutants purified from *M. smegmatis* showed similar activity to *E. coli*, as a clear indication that N-α-terminal acetylation was not present. Furthermore, mass spectrometry data conclusively reveals the state of acetylation of all proteins tested. Interestingly, acetylation was found on *E. coli* ESAT-6. Mass indicated no methionine loss, and therefore it was hypothesized the acetylation observed was resultant from another mechanism of acetylation. Trypsin digestion and subsequent search clearly proved this hypothesis true. Interestingly, other residues demonstrated clear signs of acetylation. The characterization or identification of other acetylated residues has not been implicated before and could serve as a future study. Native gel shift assay revealed a very important property from the acetylated ESAT-6. The protein does not have the same ability to deplete CFP-10 as its un-acetylated counterpart does. This clearly indicates the effect acetylation has on the

binding affinity of ESAT-6 and CFP-10. Furthermore, preliminary studies with surface plasmon resonance reveals a two-fold difference between the different types of ESAT-6

Presently, there is debate among the scientific community whether ESAT-6 enacts pH dependent membrane lysing ability or weather ESAT-6 dissociates under acidic conditions. A discrepancy between acetylated ESAT-6 and non-acetylated ESAT-6 was revealed between conflicting studies. This study demonstrates the importance of N-α-terminal acetylation in the pathogenesis of Mtb, and suggests acetylation may play a role in the dissociation of the heterodimer complex formed by CFP-10 and ESAT-6. In the present study, surface plasmon resonance revealed a difference between the binding affinities of modified or non-modified species of ESAT-6. Future studies testing for binding affinity will include a comparison between the effects acidic and neutral pH on either protein. It is expected to see a greater shift in binding affinity, with acetylated ESAT-6 binding weaker under acidic conditions as compared to a non-acetylated ESAT-6 at near neutral pH.

5.2 Conclusion

The proposition that N-α-terminal acetylation has an effect on the CFP-10 and ESAT-6 heterodimer dissociation is supported. Mutations on ESAT-6 as a complex with CFP-10 revealed no membrane lysing ability. However the very same mutations performed on lone ESAT-6 retained their activity. The intense reduction of infectivity and decreased cytosolic translocation of *M. marinum* by a single molecular process, serves as an exemplar model for possible therapeutic options to treat Mtb. Furthermore, it is observed that acetylation of the mutants is absent as indicated by NBD-Cl testing and mass spectrometry. Native gel and surface plasmon resonance revealed differential

binding between acetylated and un-acetylated ESAT-6. Therefore, N-α-terminal acetylation plays an important role in the dissociation between the CFP-10 and ESAT-6 heterodimer complex.

5.3 Future Direction

T2 of ESAT-6 appears to play an essential role in dissociation of ESAT-6 from CFP-10. The role of T2 acetylation in Mtb pathogenesis has not been well studied. Several vaccines currently in development or in testing stages are ESAT-6 based. This study provides evidence that the lack of acetylation could have a detrimental effect on the pathogenesis of TB; changing direction in the treatment development for Mtb. Current therapeutics generally target mycobacteria specific mechanisms, such as the disruption of mycolic acids by ethambutol. New treatment options in the future could include inhibitors for the acetylation of T2 at ESAT-6. More characterization is still needed underlying the process of N-α-terminal acetylation and what role this modification plays in dissociation of ESAT-6. As previously mentioned, studies testing for the different binding affinity including different pH and acetylation state would help identify discrepancies of the scientific community. The natural evolution of this study is to identifying the N- α -terminal acetyltransferase responsible for this mechanism. After identifying the enzyme, it could serve a special purpose. For example, a study to characterize it would provide with insightful information and may identify key binding sites for therapeutic targets. Similarly, plenty other post translational modifications were revealed as a result of mass spectrometry. Another possible direction could include identifying the extent of those other modifications and what their purpose is. More importantly, this study opens new doors for possible therapeutic options. The N-α-

terminal acetyltransferase for mycobacteria appears to differ from others. Since this is a particular property of this genus, then it even more possible to suggest what therapeutic options could arise. Given that a change to this solitary amino acid can disrupt the acetylation at the N-terminus, and lack of this modification causes a strong change in the phenotype of the bacteria, many possible therapeutic options could arise.

References

1. Abdallah, Abdallah M., et al. "Type VII secretion—mycobacteria show the way." Nature reviews microbiology 5.11 (2007): 883-891.
2. Acosta, Yassel, et al. "Imaging cytosolic translocation of Mycobacteria with two-photon fluorescence resonance energy transfer microscopy." Biomedical optics express 5.11 (2014): 3990-4001.
3. Augenstreich, Jacques, et al. "ESX-1 and phthiocerol dimycocerosates of *Mycobacterium tuberculosis* act in concert to cause phagosomal rupture and host cell apoptosis." Cellular Microbiology (2017).
4. Behr, M. A., et al. "Comparative genomics of BCG vaccines by whole-genome DNA microarray." Science 284.5419 (1999): 1520-1523.
5. Bernal-Perez, Lina F., Laszlo Prokai, and Youngha Ryu. "Selective N-terminal fluorescent labeling of proteins using 4-chloro-7-nitrobenzofurazan: a method to distinguish protein N-terminal acetylation." Analytical biochemistry 428.1 (2012): 13-15.
6. Braibant, Martine, and Philippe Gilot. "The ATP binding cassette (ABC) transport systems of *Mycobacterium tuberculosis.*" FEMS microbiology reviews 24.4 (2000): 449-467.
7. Brennan, Patrick J., and Hiroshi Nikaido. "The envelope of mycobacteria." Annual review of biochemistry 64.1 (1995): 29-63.
8. Brosch, Roland, et al. "Genome plasticity of BCG and impact on vaccine efficacy." Proceedings of the National Academy of Sciences 104.13 (2007): 5596-5601.
9. Brosch, Roland, et al. "Genomic Analysis Reveals Variation between *Mycobacterium tuberculosis* H37Rv and the attenuated *M. tuberculosis* H37Ra Strain." Infection and immunity 67.11 (1999): 5768-5774.
10. Casali, Nicola, and Lee W. Riley. "A phylogenomic analysis of the Actinomycetales mce operons." BMC genomics 8.1 (2007): 60.
11. Chua, Jennifer, et al. "A tale of two lipids: *Mycobacterium tuberculosis* phagosome maturation arrest." Current opinion in microbiology 7.1 (2004): 71-77.

12. Cirillo, Suat LG, et al. "Protection of *Mycobacterium tuberculosis* from reactive oxygen species conferred by the mel2 locus impacts persistence and dissemination." Infection and immunity 77.6 (2009): 2557-2567.
13. Conrad, William H., et al. "Mycobacterial ESX-1 secretion system mediates host cell lysis through bacterium contact-dependent gross membrane disruptions." Proceedings of the National Academy of Sciences (2017): 201620133.
14. Daffé, Mamadou, and Philip Draper. "The envelope layers of mycobacteria with reference to their pathogenicity." Advances in microbial physiology 39 (1997): 131-203.
15. Data and Statistics. Centers for Disease Control and Prevention. Centers for Disease Control and Prevention, 6 May 2016. Web. 16 July 2016.
16. de Jonge, Marien I., et al. "ESAT-6 from *Mycobacterium tuberculosis* dissociates from its putative chaperone CFP-10 under acidic conditions and exhibits membrane-lysing activity." Journal of bacteriology 189.16 (2007): 6028-6034.
17. De Leon, Joaquin, et al. "*Mycobacterium tuberculosis* ESAT-6 exhibits a unique membrane-interacting activity that is not found in its ortholog from non-pathogenic *Mycobacterium smegmatis*." Journal of Biological Chemistry 287.53 (2012): 44184-44191.
18. Dolin, Paul John, Mario C. Raviglione, and Arata Kochi. "Global tuberculosis incidence and mortality during 1990-2000." Bulletin of the World Health Organization 72.2 (1994): 213.
19. Fortune, S. M., et al. "Mutually dependent secretion of proteins required for mycobacterial virulence." Proceedings of the National Academy of Sciences of the United States of America 102.30 (2005): 10676-10681.
20. Gordon, Stephen V., et al. "Identification of variable regions in the genomes of tubercle bacilli using bacterial artificial chromosome arrays." Molecular microbiology 32.3 (1999): 643-655.
21. Griffin, Jennifer E., et al. "High-resolution phenotypic profiling defines genes essential for mycobacterial growth and cholesterol catabolism." PLoS Pathog 7.9 (2011): e1002251.

22. Guinn, Kristi M., et al. "Individual RD1-region genes are required for export of ESAT-6/CFP-10 and for virulence of *Mycobacterium tuberculosis*." Molecular microbiology 51.2 (2004): 359-370.
23. Hoffmann, Eik. "Patterns, Receptors, and Signals: Regulation of Phagosome Maturation." (2017).
24. Houben, Diane, et al. "ESX-1-mediated translocation to the cytosol controls virulence of mycobacteria." Cellular microbiology 14.8 (2012): 1287-1298.
25. Houben, Edith NG, Konstantin V. Korotkov, and Wilbert Bitter. "Take five—Type VII secretion systems of Mycobacteria." Biochimica et Biophysica Acta (BBA)-Molecular Cell Research 1843.8 (2014): 1707-1716.
26. Iantomasi, Raffaella, et al. "PE_PGRS30 is required for the full virulence of *Mycobacterium tuberculosis*." Cellular microbiology 14.3 (2012): 356-367.
27. Jacquez, Pedro, et al. "Expression and purification of the functional ectodomain of human anthrax toxin receptor 2 in *Escherichia coli* Origami B cells with assistance of bacterial Trigger Factor." Protein expression and purification 95 (2014): 149-155.
28. Jacquez, Pedro, et al. "The Disulfide Bond Cys255-Cys279 in the Immunoglobulin-Like Domain of Anthrax Toxin Receptor 2 Is Required for Membrane Insertion of Anthrax Protective Antigen Pore." PloS one 10.6 (2015): e0130832.
29. Kendall, S. L., et al. "The *Mycobacterium tuberculosis* dosRS two-component system is induced by multiple stresses." Tuberculosis 84.3 (2004): 247-255.
30. KOMROWER, D., & THILLAI, M. (2015). Tuberculosis and HIV co-infection. Clinical Tuberculosis: A Practical Handbook, 157.
31. Lange, Sabine, et al. "Analysis of protein species differentiation among mycobacterial low-Mr-secreted proteins by narrow pH range Immobiline gel 2-DE-MALDI-MS." Journal of proteomics 97 (2014): 235-244.
32. Ma, Yue, Verena Keil, and Jianjun Sun. "Characterization of *Mycobacterium tuberculosis* EsxA Membrane Insertion ROLES OF N-AND C-TERMINAL FLEXIBLE ARMS AND CENTRAL HELIX-TURN-HELIX MOTIFmla ci" Journal of Biological Chemistry 290.11 (2015): 7314-7322.

33. Mahairas, Gregory G., et al. "Molecular analysis of genetic differences between Mycobacterium bovis BCG and virulent M. bovis." Journal of bacteriology 178.5 (1996): 1274-1282.
34. Matthias, I., et al. "Recombinant BCG Expressing ESX-1 of *Mycobacterium marinum* Combines Low Virulence with Cytosolic Immune Signaling and Improved TB Protection."
35. McKinney, John D., et al. "Persistence of *Mycobacterium tuberculosis* in macrophages and mice requires the glyoxylate shunt enzyme isocitrate lyase." Nature 406.6797 (2000): 735-738.
36. Medie, Felix Mba, et al. "Homeostasis of N-α-terminal acetylation of EsxA correlates with virulence in *Mycobacterium marinum."* Infection and immunity 82.11 (2014): 4572-4586.
37. Miner, Maurine D., et al. "Role of cholesterol in *Mycobacterium tuberculosis* infection." (2009).
38. Murphy, Helen N., et al. "The OtsAB pathway is essential for trehalose biosynthesis in *Mycobacterium tuberculosis*." Journal of Biological Chemistry 280.15 (2005): 14524-14529.
39. Okkels, Limei Meng, et al. "CFP10 discriminates between nonacetylated and acetylated ESAT-6 of *Mycobacterium tuberculosis* by differential interaction." Proteomics 4.10 (2004): 2954-2960.
40. Ouellet, Hugues, Jonathan B. Johnston, and Paul R. Ortiz de Montellano. "Cholesterol catabolism as a therapeutic target in *Mycobacterium tuberculosis*." Trends in microbiology 19.11 (2011): 530-539.
41. Pandey, Amit K., and Christopher M. Sassetti. "Mycobacterial persistence requires the utilization of host cholesterol." Proceedings of the National Academy of Sciences 105.11 (2008): 4376-4380.
42. Piddington, Debra L., et al. "Cu, Zn superoxide dismutase of *Mycobacterium tuberculosis* contributes to survival in activated macrophages that are generating an oxidative burst." Infection and immunity 69.8 (2001): 4980-4987.

43. Pym, Alexander S., et al. "Loss of RD1 contributed to the attenuation of the live tuberculosis vaccines *Mycobacterium bovis* BCG and *Mycobacterium microti*." Molecular microbiology 46.3 (2002): 709-717.
44. Pym, Alexander S., et al. "Recombinant BCG exporting ESAT-6 confers enhanced protection against tuberculosis." Nature medicine 9.5 (2003): 533-539.
45. Refai, Amira, et al. "Two distinct conformational states of *Mycobacterium tuberculosis* virulent factor early secreted antigenic target 6 kDa are behind the discrepancy around its biological functions." Febs Journal 282.21 (2015): 4114-4129.
46. Renshaw, Philip S., et al. "Conclusive Evidence That the Major T-cell Antigens of the *Mycobacterium tuberculosis* Complex ESAT-6 and CFP-10 Form a Tight, 1: 1 Complex and Characterization of the Structural Properties of ESAT-6, CFP-10, and the ESAT-6· CFP-10 Complex IMPLICATIONS FOR PATHOGENESIS AND VIRULENCE." Journal of Biological Chemistry 277.24 (2002): 21598-21603.
47. Renshaw, Philip S., et al. "Structure and function of the complex formed by the tuberculosis virulence factors CFP-10 and ESAT-6." The EMBO journal 24.14 (2005): 2491-2498.
48. Rindi, Laura, et al. "Involvement of the *fadD33* gene in the growth of *Mycobacterium tuberculosis* in the liver of BALB/c mice." Microbiology 148.12 (2002): 3873-3880.
49. Rosenberg, Oren S., et al. "Substrates control multimerization and activation of the multi-domain ATPase motor of type VII secretion." Cell 161.3 (2015): 501-512.
50. Rotherham, Lia Suzanne. Isolation and characterization of novel aptamers against the CFP-10/ESAT-6 heterodimer for the development of TB diagnostic tools. Diss. University of Pretoria, 2012.
51. Scroggins, Bradley T., et al. "An acetylation site in the middle domain of Hsp90 regulates chaperone function." Molecular cell 25.1 (2007): 151-159.
52. Segal, William, and Hubert Bloch. "Biochemical differentiation of *Mycobacterium tuberculosis* grown in vivo and in vitro." Journal of bacteriology 72.2 (1956): 132.

53. Senaratne, Ryan H., et al. "Expression of a Gene for a Porin-Like Protein of the OmpA Family from *Mycobacterium tuberculosis* H37Rv." Journal of Bacteriology 180.14 (1998): 3541-3547.
54. Simeone, Roxane, Daria Bottai, and Roland Brosch. "ESX/type VII secretion systems and their role in host–pathogen interaction." Current opinion in microbiology 12.1 (2009): 4-10.
55. Smith, Jennifer, et al. "Evidence for pore formation in host cell membranes by ESX-1-secreted ESAT-6 and its role in *Mycobacterium marinum* escape from the vacuole." Infection and immunity 76.12 (2008): 5478-5487.
56. Sørensen, Anne L., et al. "Purification and characterization of a low-molecular-mass T-cell antigen secreted by *Mycobacterium tuberculosis*." Infection and immunity 63.5 (1995): 1710-1717.
57. Stoop, Esther JM, Wilbert Bitter, and Astrid M. van der Sar. "Tubercle bacilli rely on a type VII army for pathogenicity." Trends in microbiology 20.10 (2012): 477-484.
58. Sun, Jim, et al. "Mycobacterial nucleoside diphosphate kinase blocks phagosome maturation in murine RAW 264.7 macrophages." PLoS One 5.1 (2010): e8769.
59. Takaki, Kevin, et al. "Evaluation of the pathogenesis and treatment of *Mycobacterium marinum* infection in zebrafish." Nature protocols 8.6 (2013): 1114-1124.
60. Tan, Tracy, et al. "The ESAT-6/CFP-10 secretion system of *Mycobacterium marinum* modulates phagosome maturation." Cellular microbiology 8.9 (2006): 1417-1429.
61. TB drug resistance types. World Health Organization. World Health Organization, n.d. Web. 16 July 2016.
62. Treatment for TB Disease. Centers for Disease Control and Prevention. Centers for Disease Control and Prevention, 11 Aug. 2016. Web. 16 July 2016.
63. Tuberculosis (TB). World Health Organization. World Health Organization, n.d. Web. 16 July 2016.
64. Udwadia, Zarir F., et al. "Totally drug-resistant tuberculosis in India." Clinical Infectious Diseases 54.4 (2012): 579-581.

65. van der Wel, Nicole, et al. "*M. tuberculosis* and *M. leprae* translocate from the phagolysosome to the cytosol in myeloid cells." Cell 129.7 (2007): 1287-1298..
66. Velayati, Ali Akbar, et al. "Emergence of new forms of totally drug-resistant tuberculosis bacilli: super extensively drug-resistant tuberculosis or totally drug-resistant strains in Iran." Chest Journal 136.2 (2009): 420-425.
67. Venturini, Elisabetta, et al. "Tuberculosis and HIV co-infection in children." BMC infectious diseases 14.1 (2014): S5.
68. Vergne, Isabelle, et al. "*Mycobacterium tuberculosis* phagosome maturation arrest: mycobacterial phosphatidylinositol analog phosphatidylinositol mannoside stimulates early endosomal fusion." Molecular biology of the cell 15.2 (2004): 751-760.
69. Voskuil, Martin I., et al. "Inhibition of respiration by nitric oxide induces a *Mycobacterium tuberculosis* dormancy program." Journal of Experimental Medicine 198.5 (2003): 705-713.
70. Voskuil, Martin I., et al. "The response of *Mycobacterium tuberculosis* to reactive oxygen and nitrogen species." Frontiers in Microbiology 2 (2011): 105.
71. Watson, Robert O., Paolo S. Manzanillo, and Jeffery S. Cox. "Extracellular *M. tuberculosis* DNA targets bacteria for autophagy by activating the host DNA-sensing pathway." Cell 150.4 (2012): 803-815.
72. Wirth, Samantha E., et al. "Polar assembly and scaffolding proteins of the virulence-associated ESX-1 secretory apparatus in mycobacteria." Molecular microbiology 83.3 (2012): 654-664.
73. Wolfe, Lisa M., et al. "Proteomic definition of the cell wall of *Mycobacterium tuberculosis*." Journal of proteome research 9.11 (2010): 5816-5826.
74. Wong, Dennis, et al. "*Mycobacterium tuberculosis* protein tyrosine phosphatase (PtpA) excludes host vacuolar-H+–ATPase to inhibit phagosome acidification." Proceedings of the National Academy of Sciences 108.48 (2011): 19371-19376.
75. Yu, Jia, et al. "Both phthiocerol dimycocerosates and phenolic glycolipids are required for virulence of *Mycobacterium marinum*." Infection and immunity 80.4 (2012): 1381-1389.

76. Zhang, Qi, et al. "EsxA membrane-permeabilizing activity plays a key role in mycobacterial cytosolic translocation and virulence: effects of single-residue mutations at glutamine 5." Scientific Reports 6 (2016).

Vita

Born in Cd. Juarez, Mexico and raised in El Paso, Javier Aguilera has a passion for community engagement and his education. He graduated from Bowie High School in 2011 and continued to earn his Bachelors of Science in Biology with a concentration in biomedical sciences from the University of Texas at El Paso in 2014. He then joined the Master's program of Biology in 2015 and hopes to continue to earn his Ph.D. and later an MD.

During his time as an undergraduate student, he was recipient of the Top 10% scholarship, El Paso Community Foundation scholarship, Early Graduation Scholarship, selected for the Fast Track Graduate program and he was accepted into the Campus Office of Undergraduate Research Initiatives (COURI) in fall of 2013. As a result of COURI he joined Dr. Jianjun Sun's laboratory. During his time researching, he attended several conferences including the 2015 and 2016 COURI symposium, the Annual Biomedical Conference for Minority Students, the Rio Grande Branch ASM annual meeting, the Second Border Biomedical Research Symposium on Health Disparities, and American Society for Biochemistry and Molecular Biology annual meeting.

He was an active member of several organizations including the American Society of Microbiology, the Society of Advancement of Chicanos and Native Americans in Science and the American Society for Biochemistry and Molecular Biology. He was also one of the founding members for the Bowie jardin which provided the high school with a garden and has awarded scholarships through that program.

Contact Information: jaguilera5@utep.edu

This thesis was typed by Javier Aguilera.